Microsaccades in normal vision and in hemianopia after stroke

Dissertation

zur Erlangung des akademischen Grades

doctor rerum naturalium

(Dr. rer. nat.)

genehmigt durch die Fakultät für Naturwissenschaften

der Otto-von-Guericke-Universität Magdeburg

von   <u>M.Ed., Ying Gao</u>

geb. am   <u>22.05.1986</u>   in   <u>Jiangsu, China</u>

Gutachter: <u>Prof. Dr. Bernhard A. Sabel</u>

<u>Prof. Dr. Kevin Chan</u>

eingereicht am: <u>23.04.2018</u>

verteidigt am: <u>10.10.2018</u>

Für meine Mutter, Yongxin Gao

Für meine Großeltern, Zuoyun Gao und Guiqing Lv

Für Sendi

Acknowledgements

First of all, I would like to express my gratitude to my supervisor, Prof. Bernhard A. Sabel, for your support, encouragement, patience and the space you gave me to independently develop my own ideas. I'm so glad that we met in Beijing and I decided to join you to do researches within the topic of vision restoration and rehabilitation. I enjoyed my time in the lab and gained a lot of confidence to face the future. Thank you very much.

Secondly, I want to thank all the participants in my studies. Without you all, this work can never be achieved. We together discovered something new and added new possibilities to the future.

To my dear colleagues:

Dear Dr. Sylvia Prilloff and Steffi Matzke, thank you for your kind guidance and patient assistance in all these years.

Dear Dr. Petra Henrich-Noack, thank you for helping me a lot in science, study and living in Germany. Your diligence and sense of humor encouraged me.

Dear Dr. Lizbeth Cárdenas-Morales, thank you for all those inspiring discussions and suggestions about my study and career.

Dear Dr. Michal Bola, Dr. Carolin Gall, Dr. med. Ting Li and Dr. Elena Sergeeva, thank you all for your help and support when I was new to the lab and trying to developing my own project.

Dear Mr. Carl Huber, Ms. Sandra Heinrich, Ms. Nicole Mäter, Ms. Doreen Brösel, Ms. Anne Müller, and Ms. Eileen Poloski, I am so lucky to have your support during study conduction and data management. Thank you.

Dear Ms. Lisa Grigartzik, although we are working in different subgroups, you didn't hesitate to help me the moment I needed. I sincerely appreciate that a lot.

And many thanks to my dear fellows, Ms. Qing You, Ms. Zheng Wu, Ms. Enqi Zhang, Ms. Jiaqi Wang, Ms. Mariya Merzhvinskaya, Ms. Barbara Maria Matteo, Mr. Jiahua Xu, Mr. Xiwei Zhang, Mr. Raimund Alber, Mr. Younes Tabi, Mr. Carl Huber, Mr. Anton Kresinsky, Mr. Mohamed Tawfik and Mr. Robin Richter. You made my doctoral study colorful.

I also would like to thank Prof. Dr.-Ing. Hermann Hinrichs (Department of Neurology, Medical Faculty, Otto-von-Guericke University of Magdeburg) and Prof. Dr. Reinhold Kliegl (Department of Psychology, University of Potsdam) for their valuable comments and suggestions for my papers.

During my study, I received Performance-Oriented Granting of Funding (Leistungsorientierte Mittelvergabe) in the Faculty of Medicine at Otto-von-Guericke University of Magdeburg and Graduation Aid for international PhD students at Otto-von-Guericke University of Magdeburg. I appreciate the support from the University and the state.

Finally, I am very grateful to my dear mother and my grandparents. Thank you for encouraging me to pursue my dream. Thank you for the financial and emotional support. And thank you, Sendi, for everything.

Abstract

Vision is our dominant sense and eye movements play a key role in visual perception. Microsaccades are fast, jerk-like eye movements that happen once or twice per second. They prevent photoreceptor adaptation and counteract image fading. Moreover, they interact with brain oscillations, which suggests that they are profoundly involved in visual perception. Microsaccades show also high clinical relevance e.g. alterations of microsaccades can cause symptoms such as diplopia, reduced visual acuity and blurred vision, which are reported in a series of ophthalmological and neurological diseases. They have potentials to serve as biomarkers in diagnosis, disease monitoring and rehabilitation. The study aimed to assess microsaccades' physiological responses and their parameters across the life span so as to further understand their function in visual perception and to evaluate their potential as biomarkers in different diseases with oculomotor symptoms. I was also interested in whether microsaccades are altered in hemianopia after stroke, a disease with microsaccade-related symptoms.

The investigation comprised three studies. Study I revealed that microsaccade and microsaccade-related potentials were stable in normal aging. This suggests the usefulness of microsaccades as a potential biomarker to monitor and better understand different diseases with oculomotor symptoms. Study II revealed that microsaccades induced occipital alpha band perturbation, enhanced global alpha band cortical synchrony and increased local and global efficiency of the alpha-band functional network. I propose a mechanism of cortical refreshment: by synchronizing alpha band phase globally and by enhancing communication efficiency of the alpha band brain functional network, microsaccades can prepare the brain to optimize subsequent visual processing. Study III showed that microsaccades were enlarged in amplitude, prolonged in duration and impaired in their binocular conjugacy. These alterations were more severe in patients with older lesions. In addition, patients with a greater number of binocular microsaccades and slower microsaccade velocity performed better in visual acuity tests. Half of the patients showed a microsaccade direction bias towards the

seeing field and exhibited faster stimulus detection in areas of residual vision. These findings justify microsaccade testing as part of the routine visual function assessments in hemianopia. Future methods are needed to monitor or modulate microsaccades to open new avenues for vision restoration and rehabilitation.

To sum up, the present series of studies revealed (i) a new mechanism of microsaccades' role in visual perception, (ii) stability of microsaccades and microsaccade-related potentials across lifespan in healthy subjects, (iii) a potential use of microsaccades as biomarkers in diseases with oculomotor symptoms, (iv) that microsaccades are altered in hemianopia after stroke and some alterations can be a sign of adaptation/compensation. This supports the idea that microsaccdes should be taken into consideration in diagnosis and rehabilitation for hemianopia after stroke.

Zusammenfassung

Das Sehen ist unser dominanter Sinn und Augenbewegungen spielen eine große Rolle für die visuelle Wahrnehmung. Mikrosakkaden sind schnelle, ruckartige Augenbewegungen, die ein- oder zweimal pro Sekunde vorkommen. Sie verhindern die Fotorezeptoranpassung und gleichzeitig wirken sie dem Ausbleichen des Bildes (image fading) entgegen. Darüber hinaus interagieren sie mit Gehirnschwingungen, was darauf hindeutet, dass sie tief in die visuelle Wahrnehmung involviert sind. Mikrosakkaden zeigen außerdem eine hohe klinische Relevanz. So können z. B. Veränderungen der Mikrosakkaden Symptome wie Diplopie, verminderte Sehschärfe und verschwommenes Sehen verursachen, die bei einer Reihe von ophthalmologischen und neurologischen Erkrankungen berichtet werden. Sie haben daher das Potenzial, als Biomarker in der Diagnose, Krankheitsüberwachung und Rehabilitation eingesetzt zu werden. Ziel der Studie war es, die physiologischen Reaktionen der Mikrosakkaden und ihre Parameter über die gesamte Lebensspanne hinweg zu untersuchen, um ihre Funktion in der visuellen Wahrnehmung besser zu verstehen und ihr Potenzial als Biomarker bei verschiedenen Erkrankungen mit okulomotorischen Symptomen zu bewerten. Mich interessierte auch, ob Mikrosakkaden bei Hemianopsie nach Schlaganfall verändert sind, einer Krankheit mit mikrosakkadenbedingten Symptomen. Dies deutet auf die Nützlichkeit von Mikrosakkaden als potenzielle Biomarker hin, um verschiedene Krankheiten mit okulomotorischen Symptomen zu überwachen und besser zu verstehen. Studie II ergab, dass Mikrosakkaden die occipitale EEG-alpha-Bandleistung erhöhen, die globale Alpha-Band-Kortikalsynchronität verbessern, sowie die lokale und globale Effizienz des Alpha-Band-Funktionsnetzwerks erhöhen. Ich empfehle einen Mechanismus der kortikalen Erholung: Durch die globale Synchronisation der Alpha-Band-Phase und die Verbesserung der Kommunikationseffizienz des Alpha-Band-Gehirnfunktionsnetzwerks können Mikrosakkaden das Gehirn auf die Optimierung der nachfolgenden visuellen Verarbeitung vorbereiten. Studie III zeigte, dass Mikrosakkaden in ihrer Amplitude

vergrößert, in ihrer Dauer verlängert und in ihrer binokularen Konjugation beeinträchtigt waren. Diese Veränderungen waren bei Patienten mit älteren Läsionen stärker ausgeprägt. Darüber hinaus erzielten Patienten mit einer größeren Anzahl von binokularen Mikrosakkaden und einer langsameren Mikrosakkadengeschwindigkeit bessere Ergebnisse bei Sehschärfentests. Die Hälfte der Patienten zeigte eine Verzerrung der Mikrosakkadenrichtung in Richtung des Sehfeldes und zeigte eine schnellere Reizdetektion bei ARVs. Diese Ergebnisse rechtfertigen Mikrosakkadentests im Rahmen der routinemäßigen visuellen Funktionsbeurteilung bei Hemianopie. Neue Methoden sind notwendig, um Mikrosakkaden zu überwachen oder zu modulieren, um neue Wege für die Wiederherstellung und Rehabilitation des Sehvermögens zu eröffnen.

Zusammenfassend zeigt die vorliegende Studie (i) einen neuartigen Mechanismus zur Rolle der Mikrosakkaden in der visuellen Wahrnehmung, (ii) Stabilität der Mikrosakkaden und mikrosakkadenbezogenen Potenziale über die gesamte Lebensdauer bei gesunden Probanden, (iii) eine mögliche Verwendung von Mikrosakkaden als Biomarker bei Erkrankungen mit okulomotorischen Symptomen, (iv) dass Mikrosakkaden nach einem Schlaganfall in der Hemianopie verändert werden und einige Veränderungen ein Zeichen der Anpassung/Kompensation sein können. Dies unterstützt den Gedanken, dass Mikrosakkaden bei der Diagnose und Rehabilitation von Hemianopie nach Schlaganfall berücksichtigt werden sollten.

Table of Contents

1. Introduction

1.1.   Vision and eye movements

Vision is our dominant sense, the sense that we rely on most. The brain devotes more space to processing and storing visual information than all other senses combined. Seeing is not a passive process, but an active one. In everyday life, with our eye movements we scan endless scenes, search objects of interest, and pursue them. Besides these voluntary eye movements, we also execute a lot of involuntary eye movements. Our eyes are continuously in motion. However, we see the world clearly, continuously and stably. It's not only because our brain can realign images based on information of self-movements and fill in the images when our eyes are shut, but also because some eye movements contribute to maintaining high acuity vision and clear vision. Therefore, eye movements play a key role in our vision.

1.1.1.   Visual system

Our visual system includes the eyes, optic nerve, optic chiasm, optic tract, lateral geniculate nucleus (LGN), Optic radiation, visual cortex and visual association cortex. These structures are organized hierarchically (Figure 1.1). Visual perception begins with the light reflected off the objects being refracted by the cornea and lens and reaching the retina. The retina encodes the light as a sequence of action potentials, which are transferred via the optic nerve, optic chiasm, and optic tract to the LGN. At the optic chiasm, the optic nerves from both eyes meet and the fibers from the nasal retinas cross over, whereas the fibers from the temporal retinas do not cross. Visual information then flows via the optic radiation to the primary visual cortex (V1). V1 processes basic features of the image and distributes the information to multiple extrastriate visual areas responsible for analysis of various features, e.g. color (V4) or motion (V5/MT+). These areas, together with many other brain regions responsible for attention and multisensory integration, create a large-scale brain network, which gives

rise to conscious perception. In contrast to serial and hierarchical structure of early processing stages (up to V1), processing of visual information in cortical networks is rather distributed, parallel, and recursive(E. H. de Haan & Cowey, 2011; Van Essen et al., 1992).
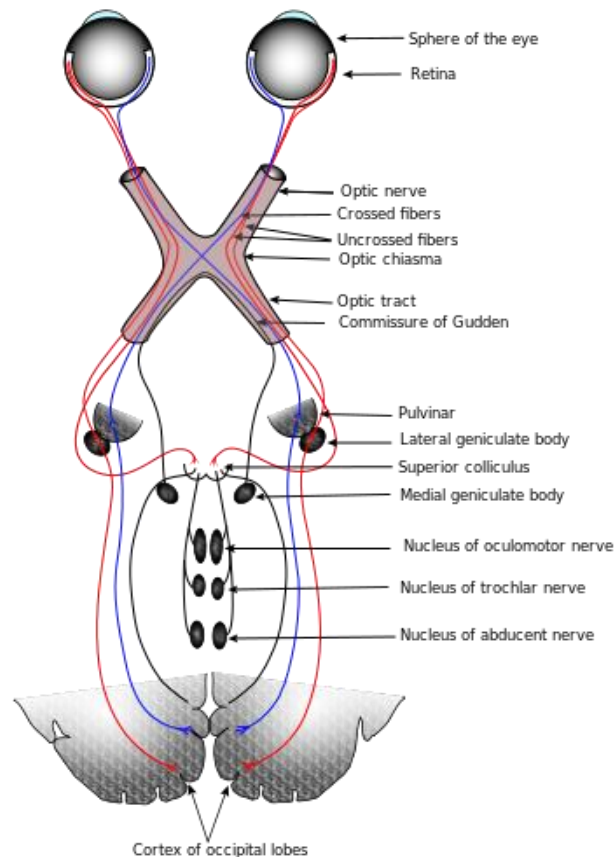
Figure 1.1. Structure of the brain visual system. Source: Wikipedia entry: visual system

1.1.2. **The eye movement repertoire and its function in vision**

Eye movements are rather sophisticated, which enables stable vision and visual analysis of fine salient details around us. *Vestibulo-ocular reflexes* are the reflexive eye movements during head movements. They stabilize the retinal image by maintaining ocular orientation and gaze stable in space. The *optokinetic reflex* is a combination of slow-phase (following a moving object) and fast-phase eye movements (moving eyes

back to the position they were in when they first saw the object). It stabilizes the image of the world on the retina during self-motion or in a moving environment. *Saccades* are fast ballistic eye movements. They direct the eyes at regions of interest, because humans' visual acuity decreases drastically away from the current location of fixation. *Ocular pursuit movements* allow us to track moving objects with a combination of *smooth pursuit movements* and *saccades*. By maintaining eye velocity close to object velocity, *smooth pursuit movements* minimize retinal image motion and maintain acuity. *Saccadic movements* help realign the retinal image if the object falls outside the retinal region of highest acuity. Lastly, even during fixation, our eyes are not absolutely still. There are three kinds of fixational eye movements, namely *microsaccades*, *tremor* and *drift*. *Microsaccades*, the biggest fixational eye movements (up to 1 degree), are small, fast and jerk-like. *Tremor* is involuntary low amplitude (< 1 min arc), high frequency ($\approx$ 90 Hz) motion of the eyes. *Drift* is slow motion ($\approx$ 6 min arc) of the eyes during the interval between microsaccades. These fixational eye movements are believed to continuously induce retinal jitter to prevent retinal stabilization (Liversedge et al., 2011). Microsaccades and their function will be discussed in section 1.3 in more detail.

1.2. Vision loss

Vision loss is the one of the most feared scenario in the elderly. Vision loss is not only an eye problem but also due to impaired neuronal processing of the retina, optic nerve and brain. Major retina and optic nerve diseases are glaucoma, optic neuritis, diabetic retinopathy and macular degeneration. Brain diseases with vision loss include middle or posterior cerebral artery stroke, brain trauma, amblyopia, and various developmental disorders. Damaging different parts of the visual system can cause different kinds of vision loss.

1.2.1. Visual system damage and visual field defects

Figure 1.2 shows the different visual field defects caused by lesions at different locations of the visual system.
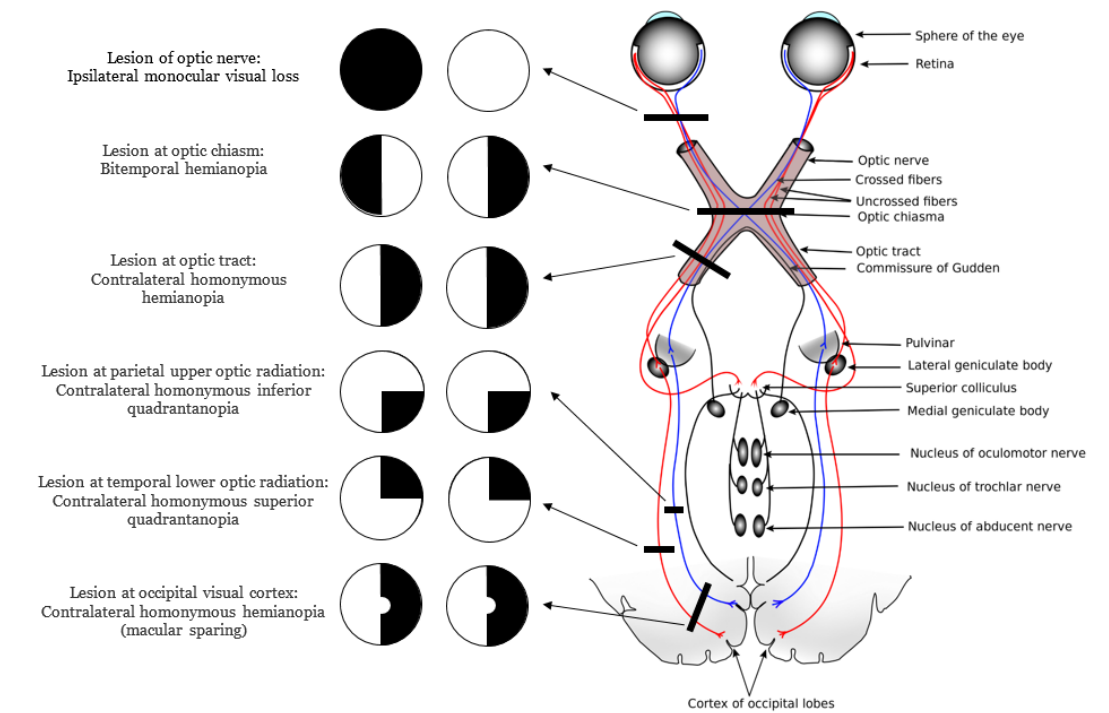
Figure 1.2. Visual field defects. *Source: Bing entry: visual field defects*

In the case of the optic nerve damage, the visual information from the corresponding eye cannot be transferred through the visual pathway, resulting in losing the visual input from the corresponding eye, analogous to losing one eye. When a lesion happens at the optic chiasm, the visual inputs from the crossing nasal fibers are lost, resulting in bitemporal hemianopia. Lesions at optic tract will block the visual input from the corresponding hemifield, causing contralateral homonymous hemianopia. Parietal upper and temporal lower optic radiations will induce contralateral homonymous inferior quadrantanopia and contralateral homonymous superior quadrantanopia respectively. Occipital visual cortex damage gives a contralateral homonymous hemianopia with macular sparing (retention of macular function in spite of losses in the adjacent visual field). In Study III in this thesis, I studied microsaccade alterations in homonymous hemianopia after stroke.

1.2.2. **Assessment of vision loss**

Below are the visual tests utilized to evaluate the extent of the vision loss.

1.2.2.1. Visual acuity test

Visual acuity tests include assessment of both near and distance vision. They measure the eye's focusing power and your ability to resolve spatial details at near and far distances. They usually involve reading letters or looking at symbols of different sizes on an eye chart (Figure 1.3).
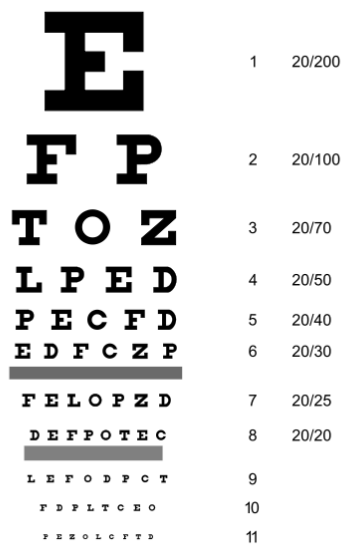
Figure 1.3. Standard Snellen chart. Source: Wikipedia entry: visual acuity

1.2.2.2. Visual field test

Visual field tests identify perceptual flaws and blind regions (scotomas) in central and peripheral vision including areas of partial damage. Perimetry is a systematic visual field test measuring light sensitivity in the whole visual field by the detection of the presence of targets on a neutral background. Subjects need to fix their gaze in order to have their visual field tested reliably.

High-resolution perimetry (HRP) is one kind of computer-based campimetric visual field test (Kasten et al., 1997). During the test, subjects need to maintain fixation at all times and press the button whenever a "target stimulus" is detected anywhere on

the screen or when the fixation point changed colour. An eye-tracker can be utilized to further control the gaze. The HRP test is performed three times. Detection accuracy in every sector of the visual field averaged over 3 testing blocks was used as a criterion to define whether a given sector of the visual field belonged to the "intact" area (100% stimuli detected, shown in white in the visual field charts, Figure 1.4), mild (66% stimuli detected, light grey) or moderate relative defect (33% stimuli detected, dark grey) or absolute defect area (0% stimuli detected, black).
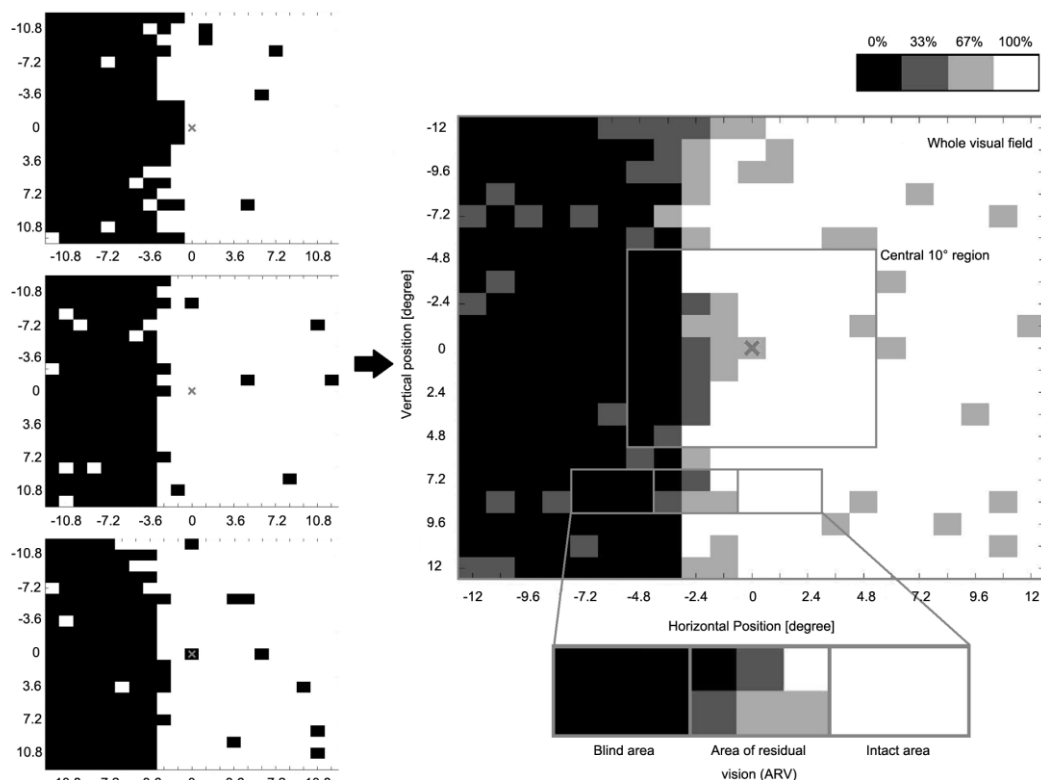
Figure 1.4. Visual area categorization based on visual field chart from high-resolution computer-based perimetry (HRP). During HRP, a supra-threshold stimulus detection task was carried out three times, creating three simple detection charts (left column). The white area shows the intact visual field, while the black area shows blind regions. By superimposing these three detection charts, we obtained a new visual chart (right center). The emerging grey area represents visual field sectors where patients' response accuracy was inconsistent; with light grey representing the area where patients responded to 2 / 3 targets and dark grey represents areas with 1/3 responses. All grey areas together are defined as

"areas of residual vision" (ARVs). The black areas and the white areas were defined as being blind or intact, respectively. As figure 1.4 shows, visual field defects are often not clear-cut, but rather fuzzy with scotomas surrounded by ARVs.

1.2.3.   Subjective feeling of the visual field defects

Decreasing visual acuity and defects in the visual field can be assessed objectively, however, they cannot capture the whole picture of vision loss. Patients' subjective feeling of the vision loss may be quite different from the visual field test results.

One reason is that the visual field defects are not as straightforward as we expected. Comparing Figure 1.5 and Figure 1.6 we can see that the visual field defect size and the topography both influence the subjective feeling of visual field loss. Symmetric defects in both eyes are easily noticed, while asymmetric defects are easily ignored because in binocular visual field, the visual image from both eyes are superimposed on each other, compensating for each other (Sabel, 2016).
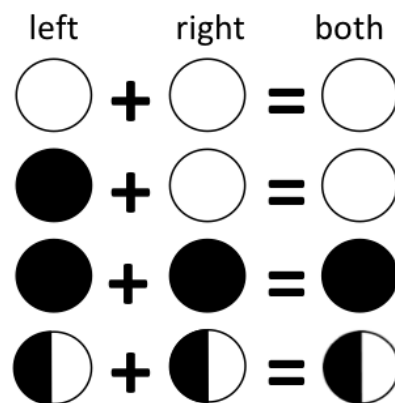
Figure 1.5. Easily noticed visual field defects. *(from Sabel, 2016, p. 55)*
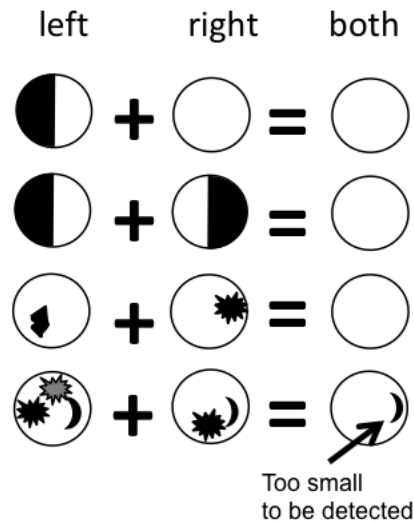
Figure 1.6. Easily ignored visual field defects. (from Sabel, 2016, p. 57)

What's more, in everyday life, we do not just view static scenes. Often times, we do not fixate at the center of the scene and stare. We actively make body, head and eye movements and receive visual information. The visual field defects at different locations have different impact on different daily tasks. Age-related macular degeneration (AMD), for example, causes a scotoma in the central visual field, which hampers a lot of tasks requiring high acuity vision such as reading. Patients are forced to turn their eyes and fixate with another preferred retinal locus (below or above the original fixation locus). Contrary to AMD, in Glaucoma and Retinitis pigmentosa, peripheral vision is affected first, gradually forming "tunnel vision". Patients will have difficulty in noticing people and cars coming from the peripheral visual field and visual search. Here, a specific scanning strategy is necessary for these patients. In hemianopia after stroke, patients lose half of the visual field. Patients with right hemi-field defects have greater difficulty in reading compared to patients with left hemi-field defects. This is because that we read from left to right and use parafoveal vision to preview the following texts.

1.2.4. Deficits in the "Intact" visual field

A lot of attention is paid to the scotoma in vision loss. Clinicians and researchers

assumed that in the "intact" field, patients' visual functions are normal. However, in addition to the "black" deficit field, the "grey" areas of residual vision (ARVs), there are even deficits in the "intact" field ("sightblindness") (Bola et al., 2013a, 2013b). Although patients with optic neuritis showed normal detection in perimetry within these "intact" fields, they exhibited impaired performance in motion detection and temporal processing tasks (Raz et al., 2011; Raz et al., 2012). Also patients suffering from homonymus hemianopia due to unilateral post-chiasmatic damage exhibit perceptual deficits in the intact field (Bola et al., 2013b), including decreased contrast sensitivity (Hess & Pointer, 1989), impaired ability to detect targets on a noisy background (Rizzo & Robin, 1996), disturbed temporal aspects of visual processing (Poggel et al., 2011), and deficits in figure-ground segregation (Paramei & Sabel, 2008; Schadow et al., 2009). Patients with pre- and post- chiasmatic visual system lesions all displayed decreased "intact" visual field processing speed (Bola et al., 2013a). To sum up, visual system lesions influence the presumed "intact" visual field as well.

1.2.5. **Other subjective visual impairments**

Besides the reduction of visual field size, there are many other poorly understood symptoms reported by patients suffering from vision loss. Take hemianopia after stroke as an example. Their vision loss is mostly described and presented by visual field chart illustrating the size and topography of the visual field defects. However, visual field size and topography correlate poorly with vision-related quality of life (Gall et al., 2010; Gall et al., 2009; Gall et al., 2008; Papageorgiou et al., 2007). In heminopia after stroke, patients often report blurred (foggy) vision and diplopia (G. A. de Haan et al., 2015; Poggel et al., 2007; Rowe et al., 2013).

To capture a comprehensive picture of vision loss in hemianopia, it is therefore necessary to identify factors contributing to subjective visual impairments. One important factor may be the quality of microsaccades.

1.3.   **Microsaccades**

1.3.1. **What are microsaccades?**

Microsaccade is one kind of fixational eye movements (Figure 1.7). They are small, fast, jerk-like eye movements produced during attempted fixation (Martinez-Conde, 2006), normally smaller than 1°, and they happen once or twice per second (Martinez-Conde, 2006; Martinez-Conde et al., 2004; Martinez-Conde et al., 2013; Otero-Millan et al., 2011a).
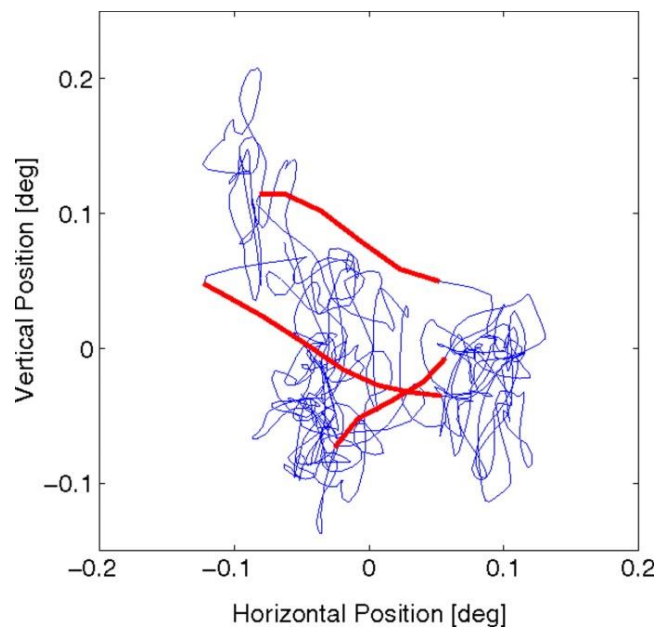
Figure 1.7. Microsaccades during attempted fixation. The trajectory shows the movements of the eye during attempted fixation. Microsaccades are marked as red.

Microsaccades and saccades are believed to be on the same continuum, sharing a common generator (Hafed & Clark, 2002; Hafed et al., 2009; Otero-Millan, Macknik, et al., 2013; Otero-Millan, Schneider, et al., 2013; Otero-Millan et al., 2008; Zuber et al., 1965). Microsaccades and saccades are both typically binocular and conjugate, and follow the main sequence. Their ballistic nature is shown in the loglog plot, exhibiting a fixed relation between microsaccade peak velocity and amplitude (Figure 1.8).
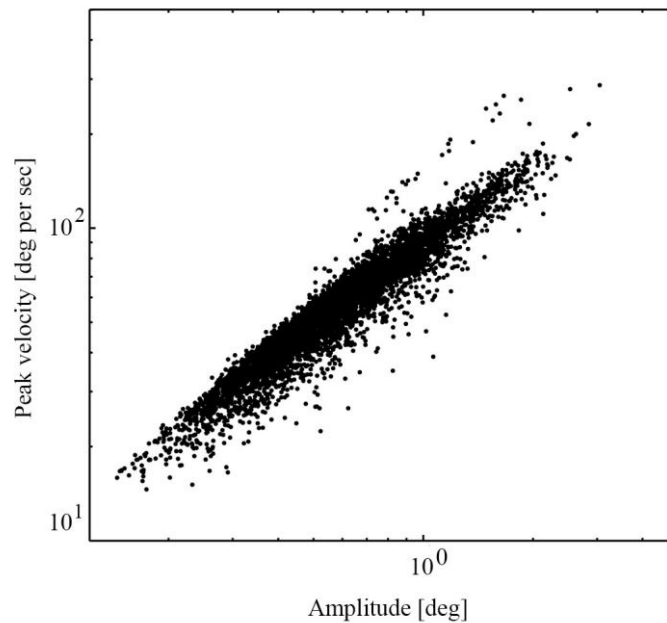
Figure 1.8. Microsaccades main sequence. *Microsaccades' ballistic nature is shown in the loglog plot, exhibiting a fixed relation between microsaccade peak velocity and amplitude.*

1.3.2. **Microsaccades' function in vision**

Microsaccades serve a series of critical functions (Martinez-Conde et al., 2013). Firstly, microsaccades are involved in oculomotor control. They introduce errors to fixation, but are corrective when the errors are too large (Otero‐Millan et al., 2011). They also correct eyeblink-introduced fixation errors (Costela et al., 2013). Secondly, Microsaccades counteract foveal and peripheral fading. By moving stimuli onto a new receptive field, which has not adapted to the stimuli, microsaccades prevent fading and restore faded vision (Martinez-Conde, 2006; McCamy et al., 2012). Thirdly, microsaccades facilitate high-acuity vision (Bridgeman & Palca, 1980; Ko et al., 2010; Poletti et al., 2013; Winterson & Collewun, 1976) and improve spatial resolution (Donner & Hemilä, 2007) during both voluntary fixation and free viewing (Benedetto et al., 2011; Otero-Millan et al., 2008). Lastly, microsaccades scan relative small and local visual fields, which is an optimal sampling strategy for the visual system to acquire information (Martinez-Conde & Macknik, 2008; Martinez-Conde et al., 2009).

Besides the above-mentioned functions, it is hypothesized that there is a mechanism underlying microsaccades to maximize information intake during fixations (Melloni et al., 2009). Microsaccade-related corollary activity was proposed to play a crucial role in anticipatory preparation of visual centers. They interact with ongoing brain oscillation, facilitating post-microsaccade visual processing.

One corollary activity is the microsaccade-induced gamma band response. However, there is a debate as to whether it represents electromyogenic artifacts or changes in cognitive processing (Nottage & Horder, 2015; Schwartzman & Kranczioch, 2011; Yuval-Greenberg et al., 2008). In fact, microsaccade-related brain activities are unlikely mere artifacts according to recent evidences that they serve as non-intrusive electrophysiological probes of attention (Meyberg et al., 2015) and that they may modulate gamma activity to facilitate visual processing and information flow between brain regions (Bosman et al., 2009; Lowet et al., 2016).

Besides the microsaccade induced gamma response, which has been repeatedly reported, there is evidence that they impact other frequency bands such as alpha band. Dimigen et al. observed several cycles of alpha ringing at occipital sites (Figure 1.9). After sorting all the trials according to the onset time of the first microsaccade in the given trial, several cycles of alpha ringing became obvious around 100 ms after microsaccade onset.

However, this phenomenon has not been examined quantitatively. In study II, I therefore studied microsaccades' interaction with alpha band oscillation utilizing different methods as now described.
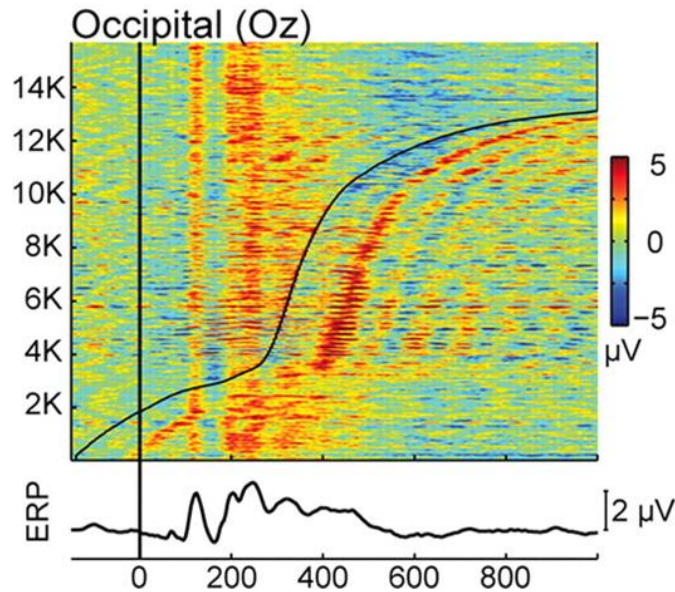
Figure 1.9. Microsaccades induced several cycles of alpha ringing at occipital sites. (from Dimigen et al., 2009)

1.3.2.1. Time frequency decomposition

Microsaccade-induced alpha band phase synchronization cannot be fully captured by event related potentials (ERPs) which probe temporal-spatial dynamics of brain activities (Herrmann et al., 2014). To overcome this limitation, we now applied time frequency analyses to characterize the microsaccade-related spectral power (event-related spectral perturbations, ERSPs) and phase (inter-trial coherence, ITC). ERSPs measure the average time course of relative changes in the spontaneous EEG amplitude spectrum induced by experimental events (Makeig, 1993). ITC, on the other hand, reflects the temporal and spectral synchronization of brain oscillatory activity, providing a direct measure of cortical synchrony (Makeig et al., 2004; Nash-Kille & Sharma, 2014).

1.3.2.2. Brain functional connectivity network analysis

Functional connectivity is the temporal correlation between spatially remote brain regions (Friston et al., 1993). It can inform us about the strength of pairwise interactions

between the brain sources that we are interested in. These interactions can be further analyzed with graph theory to exhibit brain functional network characteristics. According to graph theory, networks are represented as graphs containing nodes (brain sources) and connections between these nodes, which are called edges (Figure 1.10). Paths are sequences of linked nodes that never visit a single node more than once. The global efficiency is the average inverse shortest path length in the network. The local efficiency is the global efficiency computed on node neighborhoods (Rubinov & Sporns, 2010). These two measures provide information of the communication efficiency in the brain. On a global scale, efficiency quantifies the exchange of information across the whole brain network, while the local efficiency quantifies a network's resistance to failure on a small scale.

In a highly clustered lattice network, neighboring nodes are very well connected, resulting in high local efficiency. However, the path from one node to another remote node is quite long, which is a sign of low global efficiency. In a random network, the local efficiency is low because neighboring nodes are only randomly connected, but the global efficiency is high because the random connections between remote nodes make the long-distance connection paths shorter. A small-world network is characterized by high local and global efficiency, which is optimal for information peocessing within a system (Bassett & Bullmore, 2006; Bullmore & Sporns, 2009).
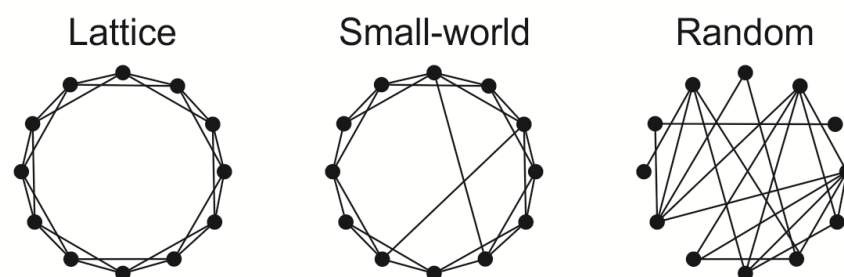
Figure 1.10. Graph nodes and edges in highly clustered lattice network, small-world network, and random network. Black dots are nodes of a graph and lines between nodes are edges.

1.4.   Microsaccades and vision loss

Microsaccades are not just important for normal cognitive visual processing but they are also clinically relevant. There are two reasons why the role of microsaccades in vision loss needs to be known.

Firstly, microsaccade alterations are closely related to subjective visual impairment, such as blurred (foggy) vision and diplopia. Too few or too small microsaccades cannot counteract central and peripheral fading, while too many or two large microsaccades lead to blurred, unstable vision (Ciuffreda & Tannen, 1995; Foroozan & Brodsky, 2004). In addition, disconjugate binocular eye movements may create diplopia.

Secondly, the control circuits of microsaccades might be interrupted in vision loss. The coordination of eye movements is controlled by multiple cortical regions such as the frontal eye field, the supplementary eye field, the prefrontal eye field, the parietal eye field, all of which are highly connected with other visual system structures (Figure 1.11) (Lynch, 2009). A microsaccade is thus a product of a successfully coordinated network. Studies have proven that in vision loss the brain functional network is disturbed, especially the occipital-frontal functional connectivity (Bola et al., 2014; Bola et al., 2015; A. R. Carter et al., 2012; Fallani et al., 2007; Grefkes et al., 2008), which synchronizes visual cortex with frontal eye fields. It is highly possible that the communication between different sectors of the microsaccade control circuits is disturbed.

Therefore, I propose that microsaccades are altered in vision loss, and to better understand vision loss, the functional status of microsaccades and their binocular conjugacy needs clarification. Below, I review the finding of microsaccade alterations in several opthalmological and neurological diseases.
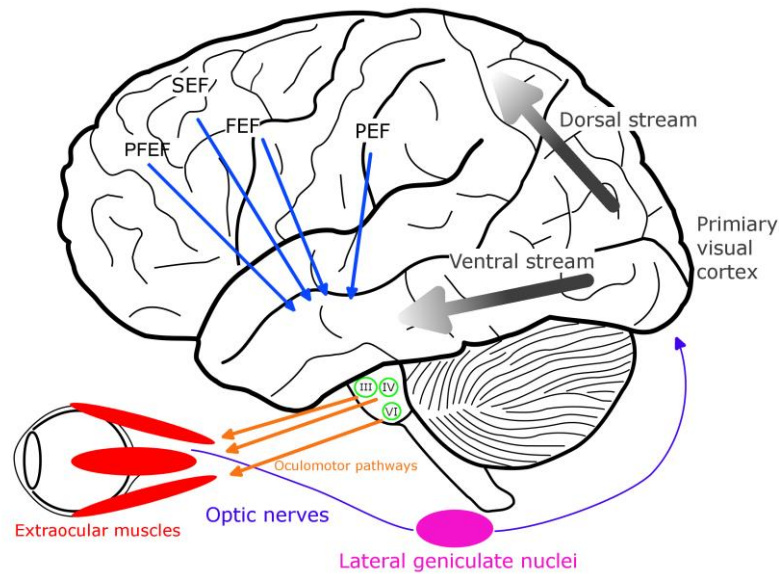
Figure 1.11. Eye movements controlled by the brain. *FEF, frontal eye field, SEF, supplementary eye field, PEF, parietal eye field. III, oculomotor nerve. IV, trochlear nerve. VI, abducens nerve.*

Microsaccades are altered in different ophthalmological and neurological diseases. In amblyopia patients, amblyopic eyes conducted fewer but larger and faster microsaccades than the control eyes (Shi et al., 2012). Shi et al. proposed that the abnormal microsaccades could be a result of the disturbed microsaccade generation under the circumstances of abnormal visual processing and circuitry reorgnization in amblyopia, but might also be an attempt of the visual system to capture more information from a broader spatial domain so as to enhance the contrast sensitivity to low spatial frequencies viewed by the amblyopic eye. Because of brainstem and/or cerebellum impairment, progressive supranuclear palsy (PSP) patients display more frequent, slowed and enlarged microsaccade amplitude and a loss of the vertical component (Otero-Millan, Schneider, et al., 2013; Otero-Millan et al., 2011b). In patients with Parkinson's disease (PD), increased fluctuations in superior colliculus (SC) activity raise the microsaccade rates, however, the brainstem and the cerebellum are relatively spared. Thus, PD patients made more frequent microsaccades than control subjects, but exhibited normal microsaccade amplitude, velocity and direction (Otero-Millan, Schneider, et al., 2013). In Alzheimer's disease (AD) and mild cognitive

impairment (MCI), altered microsaccade direction was observed, which might be related to attentional deficiencies (Kapoula et al., 2014). No alterations of microsaccade amplitude, duration and peak velocity indicated the spared brainstem saccade generator, which is consisitent with the lack of brainstem oculomotor symptoms in MCI and AD patients.

1.5. Problem formulation and hypothesis

To sum up, microsaccades' role in normal and abnormal vision requires further study. Therefore I aimed to assess microsaccades' physiological responses and their parameters across the life span so as to further understand their function in visual perception and to evaluate their potential as biomarkers in different diseases with oculomotor symptoms. I was also interested in whether microsaccades are altered in hemianopia after stroke, a disease with microsaccade-related symptoms.

1.5.1. Microsaccades and microsaccde-related potentials across the life span

Since the above-mentioned diseases displaying microsaccade alterations often occur in different age groups, we need to learn if microsaccade features are age-dependent. Although age-matched normally sighted subjects are widely used for comparison with patients, reference values for the different microsaccade features across age are still missing. Saccades - larger-type eye movements - are on the same continuum and share the same singular generator circuits with microsacacdes (Hafed & Clark, 2002; Hafed et al., 2009; Otero-Millan, Macknik, et al., 2013; Otero-Millan, Schneider, et al., 2013; Otero-Millan et al., 2008; Zuber et al., 1965). Involuntary saccades were found to be stable across different age groups (Hamel et al., 2013; Kerber et al., 2006; Peltsch et al., 2011; Pratt et al., 2006; Raemaekers et al., 2006; Yang & Kapoula, 2006), but if this is also true for microsaccades - which are also involuntary - is unknown.

In study I, I assessed microsaccades and microsaccade-related potentials in subjects aged 18-77 yrs with the hypothesis that they remain stable across the life-span

as involuntary saccades do, while the microsaccade-related potentials might change in aging.

1.5.2. Microsaccades' influences on the brain oscillation and brain functional network

Microsaccades have been proposed to interact with ongoing brain oscillation to maximize information intake during fixations (Melloni et al., 2009). Besides the microsaccade induced gamma response, which has been repeatedly reported, there is evidence that they also influence alpha band activity. Dimigen et al. reported alpha synchronization at occipital sites around 100 ms after microsaccade onset (Figure 1.9). However, this phenomenon has not been examined quantitatively.

In study II, I assessed microsaccade-related temporal-spectral power and synchronization dynamics to replicate previous finding and quantify it in spatial, temporal and spectral dimensions. To further understand the microsaccade-related alpha synchronization, I computed microsaccade-related brain functional connectivity network features, i.e. global efficiency and local efficiency to reveal microsaccades' impact on the local and global communication of the brain.

1.5.3. Microsaccades in hemianopia after stroke and their correlations to visual function

In hemianopia after stroke, visual field size and topography correlate poorly with vision-related quality of life (Gall et al., 2010; Gall et al., 2009; Gall et al., 2008; Papageorgiou et al., 2007). Besides the reduction of visual field size, patients may also experience other still poorly understood symptoms such as blurred vision, diplopia, or reduced visual acuity (G. A. de Haan et al., 2015; Poggel et al., 2007; Rowe et al., 2013). One potential contributor to these visual impairments is microsaccade alteration. Altered microsaccades can cause blurred (foggy) vision and low visual acuity (Ciuffreda & Tannen, 1995; Foroozan & Brodsky, 2004). In addition, studies have shown that brain network disturbances are responsible for functional impairments well

beyond the local lesion (Catani et al., 2012), possible connectivity alteration between the damaged visual system and cortical eye fields is to be expected in hemianopia after stroke. Therefore, to better understand vision loss in hemianopia, the functional status of microsaccades and their binocular conjugacy needs clarification.

In study III, I compared microsaccade features in hemianopia to those in healthy controls and correlated them with visual performances and lesion age. I hypothesized that patients suffering from hemianopia exhibited: (i) enlarged microsaccade amplitude due to a decreased inhibition of the SC after visual deafferentation (Shi et al., 2012); (ii) reduced binocular microsaccade conjugacy due to miscalibration of the eye movement control network after visual input deprivation (Schneider et al., 2013); and (iii) microsaccade direction bias towards the deficit side, which was reported in hemianopia (Reinhard et al., 2014).

2. Study I: Microsacade features across the life span

Published in:

Gao, Y., Huber, C., Sabel, B. A. Stable microsaccades and microsaccade-induced global alpha band phase reset across the life span. Investigative Ophthalmology & Visual Science. 59(5): 2032-2041.

2.1.   Study I: Introduction

2.1.1.   Microsaccade norm references in different age groups are necessary

Microsaccades, small, fast, and jerk-like eye movements, play a significant role in normal vision and they are altered in different ophthalmological and neurological diseases. For example, in amblyopia patients, amblyopic eyes conducted fewer but larger and faster microsaccades than the control eyes (Shi et al., 2012). Progressive supranuclear palsy (PSP) patients display more frequent, slowed and enlarged microsaccade amplitude and a loss of the vertical component (Otero-Millan, Schneider, et al., 2013; Otero-Millan et al., 2011b). In patients with Parkinson's disease (PD), patients made more frequent microsaccades than control subjects, but exhibited normal microsaccade amplitude, velocity and direction (Otero-Millan, Schneider, et al., 2013). In Alzheimer's disease (AD) and mild cognitive impairment (MCI), altered microsaccade direction was observed, which might be related to attentional deficiencies (Kapoula et al., 2014).

Since these diseases often occur in different age groups, particularly in the elderly population, it is crucial to know if microsaccades are age-dependent to appreciating the impact of these diseases on microsaccades. Although age-matched control subjects for comparison with patients is widely used, a thorough description of

microsaccade features in different age groups is still required as a references for future studies and clinical applications, which is lacked. Only one study investigated the microsaccade features during a puzzle task in subjects aged from 4 to 66 yrs and found a slightly increasing saccade frequency by age (Port et al., 2016). The present study was carried out to provide more evidence. To avoid confounding factor introduced by age-related declination in cognitive tasks (e.g. in a puzzle task), in this study a simple fixation task was utilized to investigate the microsaccade function in aging.

2.1.2. Aging effect on macrosaccades

Another kind of saccade, macrosaccade, which is on the same continuum and share the same singular saccade generator cirtuits with microsaccades (Hafed & Clark, 2002; Hafed et al., 2009; Otero-Millan, Macknik, et al., 2013; Otero-Millan, Schneider, et al., 2013; Otero-Millan et al., 2008; Zuber et al., 1965), has been investigated in aging for decades. Voluntary saccadic performances decline in elderly subjects (Abel & Douglas, 2007; Abel et al., 1983; Butler et al., 1999; J. E. Carter et al., 1983; Chen & Machado, 2016; Huddleston et al., 2014; Klein et al., 2000; Klein et al., 2005; Litvinova et al., 2011; Matiño-Soler et al., 2015; Munoz et al., 1998; Olincy et al., 1997; Sharpe & Zackon, 1987; Spooner et al., 1980; Tedeschi et al., 1988; Yang & Kapoula, 2006) while automatic saccades were found to be less affected by age (Hamel et al., 2013; Kerber et al., 2006; Peltsch et al., 2011; Pratt et al., 2006; Raemaekers et al., 2006; Yang & Kapoula, 2006). Because of these latter observations, we hypothesized that involuntary microsaccades - which are also non-voluntary - are relatively impervious to the effect of aging. We expected no change of microsaccade features in aging except a potential increase in microsaccade rate by age as reported (Port et al., 2016).

2.1.3. Microsaccade-related potentials

Besides behavioral observations, the physiology of microsaccades has been explored. There are fundamentally two typical microsaccade-locked brain potentials:

the spike potential (SP) and the microsaccadic lambda response (MLR). Whereas the SP is a summation of Electromyography (EMG) spikes at microsaccade onset, the MLR represents the occipital activation by microsaccade-caused retinal slip, which was proposed to be similar to visually evoked potentials (VEP) (Dimigen et al., 2009). Because the VEP is known to be sensitive to aging, manifested by its delays and amplitude reductions (Kuba et al., 2012), we wonder whether VEP-like MLR also changes as a function of age. This kind of analysis on amplitudes and latencies are based on ERPs technique, which averages the electroencephalogram (EEG) across a number of experimental trials and assesses the temporal-spatial dynamics of brain activities (Herrmann et al., 2014).

2.1.4. Study aim and hypothesis

We aim to assess the microsaccade features and microsaccade-related potentials in subjects aged 18-77 yrs and explore the age effect on these measures. We hypothesized that microsaccades features such as amplitude, peak velocity, binocular microsaccade percentage, binocular conjugacy are relatively impervious to the age effect, while microsaccade rate slightly increases in aging. We also hypothesized that microsaccade-related potentials, i.e. SP and MLR, might be sensitive to aging.

2.2. Study I: Methods

2.2.1. Participants

22 young subjects (aged 18-29 years, mean ± S.D. 23.8 ± 3.4 yrs, 13 female), 22 middle-aged subjects (aged 31-55 years, 45.5 ± 7.9 yrs, 13 female) and 22 elderly subjects (aged 56-77 years, 64.7 ± 5.7 yrs, 13 female) participated in this study. All subjects have normal or corrected to normal visual acuity (20/20) and no visual field deficits. A research assistant with a medical background interviewed all subjects. Exclusion criteria included a history of hemianopia, amblyopia, glaucoma, cataract, diplopia, nystagmus, cataract, PD, AD and other disorders affecting the visual and oculomotor function. Written informed consent was obtained from all participants

according to the Declaration of Helsinki (International Committee of Medical Journal Editors, 1991) after the institutional review board approved the study protocol.

2.2.2. Experimental protocol

During a fixation task, participants were instructed to maintain fixation at a fixation dot on a gamma corrected monitor (EIZO, CG241W, resolution of 2560×1440), which was placed at 67 cm distance. The white fixation dot (size: 10 pixels, luminance: 90 cd/m2) was presented against grey background (luminance: 29 cd/m2) in 40 trials lasting 7 sec each. The inter-stimulus interval was 3 sec, during which participants could rest their eyes. All participants were tested individually in a silent, dimly lit room.

2.2.3. Eye movement recording

Binocular eye movements were recorded during the fixation task using an EyeLink-1000 system (SR Research, Ontario, Canada) with a sampling rate of 500 Hz and a spatial resolution of 0.01°. Head position was stabilized via a chin and forehead rest during eye tracker calibration, validation and recording.

2.2.4. EEG recording

During the fixation task, dense array EEG was simultaneously recorded with the eye movement data, using a HydroCell GSN 128-channel net and Net Amps 300 amplifier (EGI Inc., Eugene, Oregon, USA). Our recording used a sampling rate of 500 Hz, a 200 Hz anti-aliasing low pass filter, Cz as a reference (ground electrode between Cz and Pz), and was digitalized with 24-bit precision. Impedance was kept below 100 kΩ throughout the recording. Common trigger pulses were sent from the presentation computer to both eye tracking computer and EEG recording device for offline co-registration of eye movements and EEG.

2.2.5. Data analysis

Continuous EEG signal was filtered with high-pass (1 Hz) finite impulse response (FIR) filter, low pass (100 Hz) FIR filter, and notch (50 Hz) FIR filter. Eye tracking data and EEG data were synchronized and the synchronization quality was checked manually. Out-of-range eye tracking and EEG data was removed when there was a blink or when the eyes were not focused on the fixation point centered in a 4° x 4° window. Then, we performed microsaccade detection, with a function implemented based on the algorithm for microsaccade detection proposed by Engbert and colleagues (Engbert & Kliegl, 2003; Engbert & Mergenthaler, 2006). The time series of eye positions were transformed to velocities by calculating a moving average of velocities over five data samples. A microsaccade was defined by the following criteria: (i) the velocity exceeded six median-based standard deviations of the velocity distribution; (ii) the duration exceeds 12 msec (6 data samples); (iii) the inter-saccadic interval exceeded 50 msec (25 data samples), otherwise only the largest microsaccade would be kept. Then, binocular microsaccades were defined as those that occurred in left and right eyes with a temporal overlap. We collected different microsaccade features such as rate (microsaccade number divided by detection time window length), amplitude (the Euclidean distance between the start and end point of the movement), velocity (the peak velocity during one microsaccade), duration, binocular microsaccade percentage (the proportion of binocular microsaccades in all detected microsaccades), horizontal and vertical binocular disconjugacy indices (Gao & Sabel, 2017).

After this analysis binocular microsaccades were added as "events" into the EEG data, epochs locked to them [−0.5 s to 0.5 s] were extracted and baseline corrected [−0.2 s to 0 s]. Epochs were manually screened for artifacts and noisy channels (on average 70.1 ± 85.1 epochs per subject discarded; 7.4 ± 5.2 channels per subject discarded and interpolated based on the activity of surrounding channels). On average, 117.9 ± 17.5 epochs in the young group, 147.1 ± 75.1 epochs in the middle-aged group, and 137.9 ± 19.4 epochs in the elderly group were analyzed. We analyzed two typical microsaccade-related potentials, e.g. MLR and SP. Potential latencies were defined in grand averaged ERPs for each of the three groups. Within a short window around it (20ms for MLR;

10ms for SP), individual potential amplitude and latencies were located. Representative electrodes were selected for the occipital region (E75, E70, E83), central region (E7, E31, E55, E80 and E106) and frontal region (E11, E19, E4) (Figure 2.1).
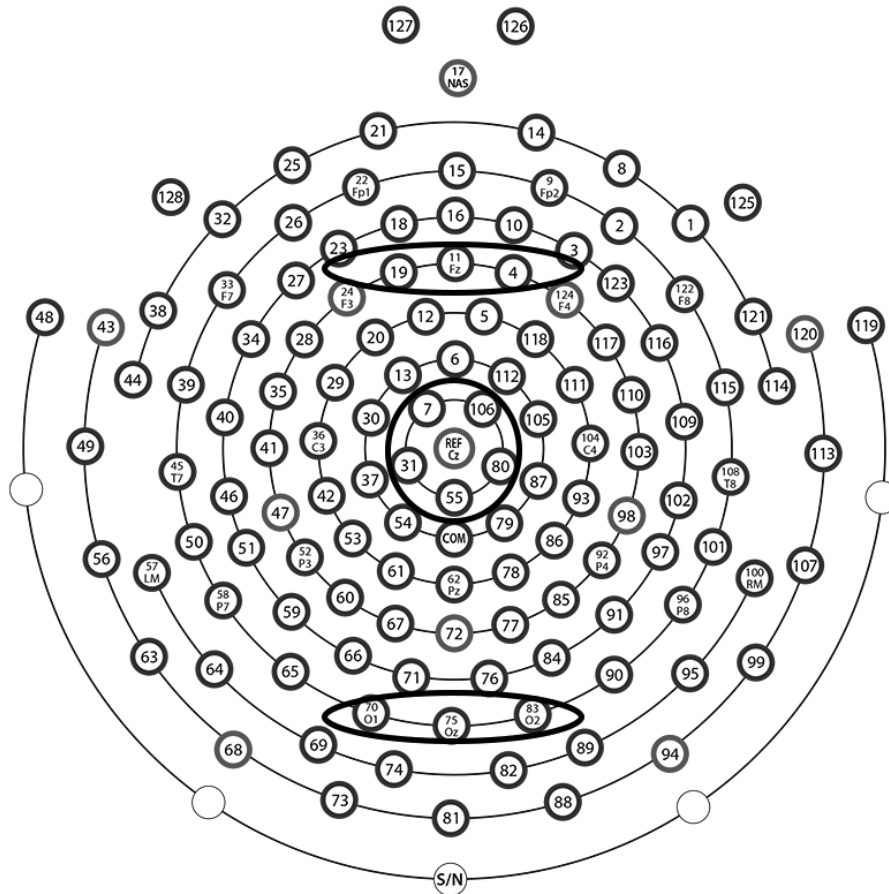
Figure 2.1. Locations of electrodes selected for the occipital (E75, E70, E83), central (E7, E31, E55, E80 and E106) and frontal regions (E11, E19, E4).

2.2.6. Statistics

ANOVA was used to test age effect on microsaccade features (binocular microsaccade percentage, microsaccade rate, amplitude, velocity, duration, horizontal and vertical disconjugacy indices), the amplitudes and latencies of SP and MLR. Before conducting between-groups statistical tests, normality of distribution was assessed with Kolmogorov-Smirnov test of normality. For measures violating the normal distribution

assumption, Kruskal-Wallis test was used. To correct for multiple comparisons (9 comparisons conducted), a criterion of P = 0.005 (two-tailed) was set according to Bonferroni correction.

2.2.7. **Software**

The experiment was developed in SR research Experiment Builder. Data analysis was conducted using Matlab 2016 and the following open-access toolboxes: EEGlab (Delorme & Makeig, 2004), EYE-EEG extension (http://www2.hu-berlin.de/eyetracking-eeg) (Dimigen et al., 2011). Statistical analyses were performed using IBM SPSS Statistics 23 (IBM, USA, http://www.ibm.com/software/analytics/spss/).

2.3. **Study I: Results**

2.3.1. **Microsaccade features**

Figure 2.2 displays the main sequences and angular distributions of microsaccades in three age groups. The main sequences for the three age groups were similar and the microsaccade orientations exhibited a similar horizontal preference in three age groups, which is typical in normal subjects (Dimigen et al., 2009).
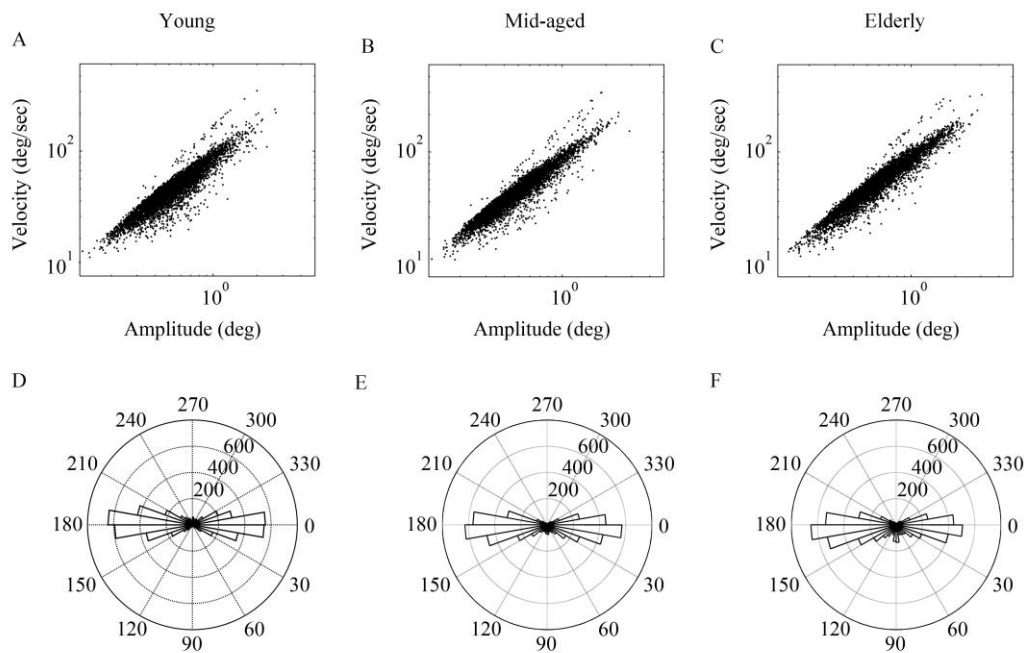
Figure 2.2. Microsaccade main sequences (A: young; B: middle-aged; C: elderly) and angular histograms (D: young; E: middle-aged; F: elderly). Note: Bar length in the angular histograms represents microsaccade numbers.

Microsaccade and microsaccade-related potential features in the three age groups are shown in Table 2.1. ANOVA revealed all microsaccade features to be comparable between the three groups, except that the elderly group showed higher microsaccade velocity compared to the young group (P =0.017). But this difference did not survive Bonferroni correction. Figure 2.3 illustrates the distribution of each microsaccade feature in three age groups with horizontal lines indicating 5% and 95% percentiles.

Table 2.1. Microsaccade features in different age groups

	18-30 yrs		31-55 yrs		56-77 yrs		F	p
	Mean	SD	Mean	SD	Mean	SD		
Microsaccade							df (2,65)	
Binocular microsaccade percentage (%)	41.21	7.99	42.11	7.93	43.02	5.39	1.25*	0.536
Rate (n/sec)	1.24	0.70	1.31	0.60	1.43	0.72	0.77	0.469
Amplitude (deg)	0.51	0.14	0.48	0.10	0.57	0.14	2.17	0.123
Velocity (deg/sec)	52.81	14.52	52.30	11.04	62.15	12.84	4.36	0.017
Duration (sec)	19.85	2.82	21.03	2.11	21.00	3.26	2.11	0.130
Horizontal disconjugacy (min arc)	5.77	1.42	5.78	1.24	6.46	2.29	0.33*	0.846
Vertical disconjugacy (min arc)	7.12	2.14	6.87	1.67	8.00	2.27	2.18*	0.337

* Kruskal-Wallis test was used and Chi-Square values reported due to violation of the normal distribution assumption. Degree of freedom was 2.

MLR = microsaccadic lambda response, SP = spike potential.

To correct for multiple comparisons, a criterion of P = 0.005 (two-tailed) was set for the ANOVAs according to Bonferroni correction.
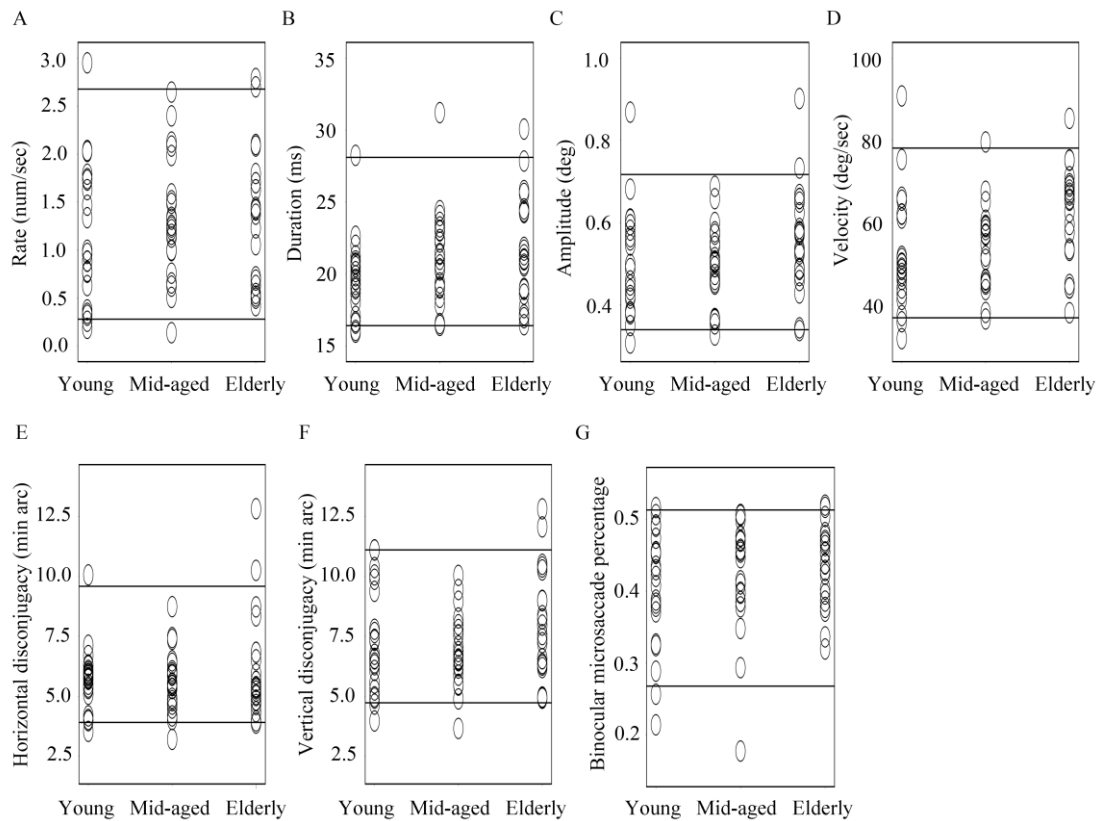
Figure 2.3. Scatter plots of microsaccade features of the three age groups. *Distributions of microsaccade rate (A), duration (B), amplitude (C), velocity (D), horizontal (E) and vertical disconjugacy (F), and binocular microsaccade percentage (G); horizontal lines mark the 5% and 95% values of the respective distributions.*

2.3.2. **Microsaccade-related potentials**

Microsaccade and microsaccade-related potential features in the three age groups are shown in Table 2.2. ANOVA revealed all microsaccade features to be comparable between the three groups, except that the elderly group showed higher microsaccade velocity compared to the young group (P =0.017). But this difference did not survive Bonferroni correction.

Table 2.2. Microsaccade-related potential features in different age group

	18-30 yrs		31-55 yrs		56-77 yrs			
	Mean	SD	Mean	SD	Mean	SD	F	p
MLR							df (2.53)	
Amplitude (μV)	2.63	1.28	2.24	1.77	2.22	1.48	0.47	0.650
Latency (ms)	159.34	12.61	157.29	8.20	160.89	7.00	0.61	0.549
SP							df (2.53)	
Amplitude (μV)	1.40	1.32	1.02	0.96	0.97	1.04	0.79	0.461
Latency (ms)	15.63	2.20	14.85	2.50	14.85	2.24	0.71	0.495

To correct for multiple comparisons, a criterion of P = 0.005 (two-tailed) was set for the ANOVAs according to Bonferroni correction

Figure 2.4 shows the grand average ERPs of three age groups at occipital and central regions, the scalp distributions and the current density maps of the SP and MLR. SP began around -5ms before microsaccade onset and peaked around 16ms after microsaccade onset. The scalp distribution of the SP displayed a positive deflection at central and occipital regions and negative deflection at the frontal region. The visualization of the source estimation result displayed a high current density in the anterior region close to the eyes. MLR began around 120ms and peaked around 160ms after microsaccade onset. The scalp distribution of the MLR exhibited a positive deflection occipitally and a negative deflection centrally. The visualization of the source estimation result displayed a high current density in the posterior part of the brain. ANOVA results revealed no significant differences in the latencies and amplitudes of the SP and MLR between the three groups.
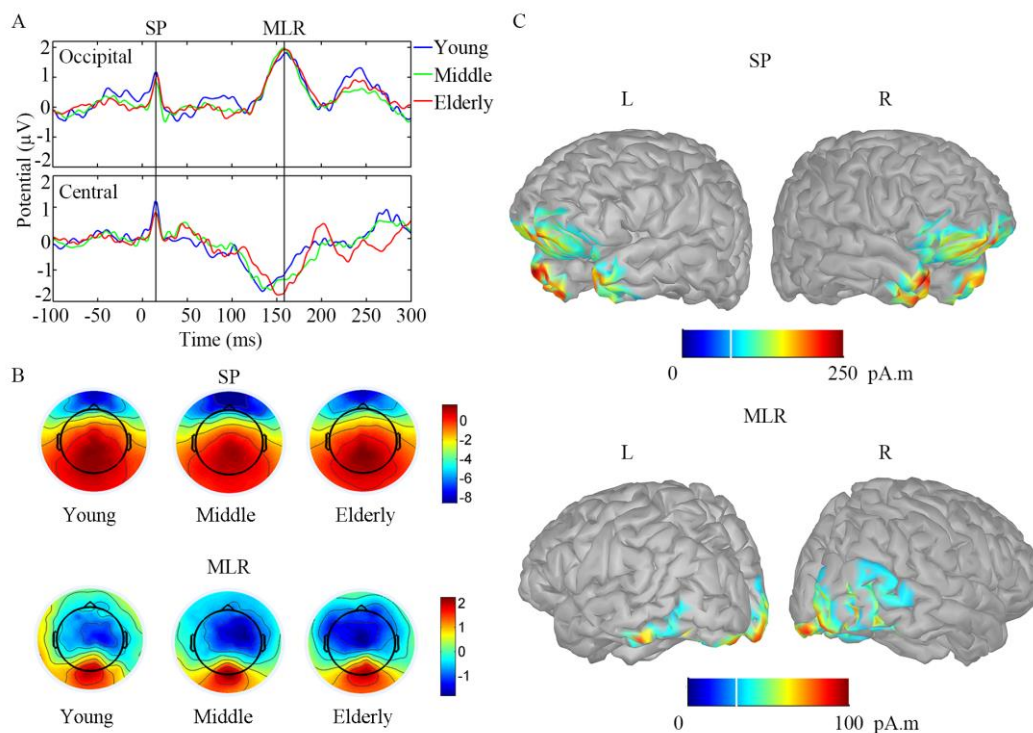
Figure 2.4. Average ERPs of three age groups at occipital region and central region (A), the scalp distributions (B) and the current density maps (C) at spike potential (SP) peak and microsaccadic lambda response (MLR) peak. Black vertical lines in panel A mark the peak of SP and MLR.

2.4.   Study I: Discussion

We report the first comprehensive assessment of microsaccade features and microsaccade-related potentials in a group of 66 subjects of ages between 18 and 77 yrs. Microsaccade and microsaccade-related potential features were found to remain stable across the life span.

2.4.1.   Microsaccades across the life span

All microsaccade features (binocular microsaccade percentage, microsaccade rate, amplitude, velocity, duration, horizontal and vertical binocular disconjugacy) were comparable between the three age groups. This is compatible with what is known about involuntary saccades, which, unlike voluntary saccades, were relatively impervious to aging. This implies that while voluntary saccade function declines with age, involuntary saccade function does not (Peltsch et al., 2011). As we now showed, this is true also for the involuntary microsaccades: subjects ranging in age from 18 to 77 yrs showed similar abilities to generate microsaccades and maintain binocular coordination.

Our results are not at odds with another seemingly contradictory report, which investigated microsaccade features during a puzzle solving task in subjects of different ages (4 to 66 yrs) where slightly increasing microsaccade rates were reported with increasing age (Port et al., 2016). We did not observe such change, which might be due to the differences in the experimental tasks. We believe that the cognitive load of the puzzle task, which is sensitive to aging, might interact with microsaccade rate modulation. In contrast, we used a simple fixation task to avoid any cognitive load. In fact, it is known that elderly subjects perform worse in relatively difficult eye movement tasks requiring inhibition, high attention demand or wider attention span (Campbell et al., 2009; Gottlob et al., 2007; Huddleston et al., 2014).

The slightly higher microsaccade velocity in our elderly group should be considered as preliminary evidence as it was not significant after Bonferroni correction. We briefly discuss it here as a reference for future studies. Studies about age effects on

saccade velocity exhibited a discordant variety of findings. Whereas some studies revealed no age effect on saccade peak velocity (Abel et al., 1983; Hamel et al., 2013; Kerber et al., 2006; Munoz et al., 1998; Pratt et al., 2006; Spooner et al., 1980; Yang & Kapoula, 2006), others discovered reduced velocity in the elderly population, especially in larger (>20°) saccades (Moschner & Baloh, 1994; Pitt & Rawles, 1988; Schik et al., 2000; Sharpe & Zackon, 1987; Sweeney et al., 2001; Warabi et al., 1984; Wilson et al., 1993). Similar to our findings, some elderly subjects made faster saccades than the young ones, but the statistical results suggested no significant age effect on saccade velocity when conducting the group comparison (Abel et al., 1983). Future studies with larger samples of elderly subjects are needed to clarify this issue.

2.4.2. Microsaccade-related potentials across the life span

We also analyzed the typical microsaccade-related potentials across the life span. Figure 2. 4 displays the averaged ERPs in the occipital and central regions, with time locked to microsaccade onset. SP is the spike peaking at about 16 ms after microsaccade onset, which has a positive deflection at central and occipital regions and negative deflection at the frontal region. It is the summation of the EMG signals accompanying microsaccade execution, which is further confirmed by its high current density near the eyes. MLR is the potential peaking at about 160 ms after microsaccade onset. It has positive polarity at the occipital and negative polarity at the vertex. At the MLR peak, high current density was found in the occipital lobe. MLR represents the occipital activation by microsaccade-induced retinal image slip, which resembles the VEP. In the Dimigen study, the MLR peaked at 100 ms after microsaccade onset with a mean amplitude of 9.6 µV (Dimigen et al., 2009). In our study, however, MLR peaked at 160 ms after microsaccade onset with mean amplitude of 2.4 µV. This difference could be due to the different stimuli. Whereas we used a white dot presented against a grey background, Dimigen and colleagues used a black-and-white checkerboard. More intense visual stimuli can enlarge VEP amplitude and shorten their latency (Connolly & Gruzelier, 1982). We therefore believe that the less demanding stimuli used in our study resulted in smaller occipital activation caused by microsaccadic retinal slip,

generating smaller MLR amplitude and longer MLR latency. Considering the age effect, we found that - like the behavioral microsaccade features - the amplitudes and latencies of the SP and MLR were stable across the life span.

2.5.   Study I: Conclusion

We found that microsaccade and microsaccade-related potentials were stable across the life span. This stability is an excellent condition so that microsaccades can serve as reference points when studying age-associated neurodegenerative or neuro-ophthalmological diseases with oculomotor symptoms. This suggests the usefulness of microsaccades as a potential biomarker to monitor and better understand different diseases with oculomotor symptoms.

3. Study II: Microsaccades induce global alpha band phase reset and alpha band network efficiency enhancement

Published in:

3.1. Study II: Introduction

Microsaccades are small, fast, and jerk-like eye movements that refresh vision by preventing photoreceptor adaptation, and scan relative small and local visual fields (Martinez-Conde et al., 2013). In addition, their corollary activities might also interact with ongoing brain oscillation to prepare visual centers for upcoming stimuli (Melloni et al., 2009). Though one corollary activity is the microsaccade-induced gamma band response, there is a debate as to whether it represents electromyogenic artifacts or changes in cognitive processing (Nottage & Horder, 2015; Schwartzman & Kranczioch, 2011; Yuval-Greenberg et al., 2008). However, microsaccade-related brain activities are unlikely mere artifacts according to recent evidences that they serve as non-intrusive electrophysiological probes of attention (Meyberg et al., 2015) and that they may modulate gamma activity to facilitate visual processing and information flow between brain regions (Bosman et al., 2009; Lowet et al., 2016).

Another microsaccade-related corollary activity is within the alpha band. Around 100 ms after microsaccades, alpha phase synchronization at occipital sites were observed (Dimigen et al., 2009). It has been proposed that top-down alpha phase interactions can achieve the reconciliation of inhibiting task-irrelevant information and

active processing of task-relevant information (Palva & Palva, 2011). Microsaccade-related alpha phase synchronization is of great interest to understanding microsaccades' function in visual perception. However, this phenomenon has not been studied quantitatively and cannot be fully captured by averaged ERPs which probe temporal-spatial dynamics of brain activities (Herrmann et al., 2014). To overcome this limitation, we now applied time frequency analyses to characterize the microsaccade-related spectral power (event-related spectral perturbations, ERSPs) and phase (inter-trial coherence, ITC). ERSPs measure the time course of relative changes in the spontaneous EEG amplitude spectrum induced by experimental events (Makeig, 1993). ITC, a measure of cortical synchrony, on the other hand, reflects the temporal and spectral synchronization of brain oscillatory activity (Makeig et al., 2004; Nash-Kille & Sharma, 2014). Besides occipital region, the alpha phase dynamics of frontal and central regions are also of interest in this study. Large-scale networks of inter-areal interactions exist in the alpha band. It has been suggested that inter-areal alpha-band phase interactions in the fronto-parietal regions may underlie the top-down modulation of local oscillation amplitudes in sensory regions (Palva & Palva, 2011). How microsaccade interact with this alpha band network is still unclear. In this study, functional connectivity between different brain sources were evaluated and the local and global efficiency of microsaccade-related brain functional connectivity network were assessed based on graph theory. These two measures provide information of the communication efficiency in the brain. On a global scale, efficiency quantifies the exchange of information across the whole brain network, while the local efficiency quantifies a network's resistance to failure on a small scale.

To this end, I aimed to quantify microsaccade-related temporal-spectral power, phase synchronization dynamics and brain functional connectivity network characteristics to learn more about microsaccades' impact on brain activity.

3.2.   Study II: Methods

3.2.1.   Participants

22 young (18-29 yrs, mean ± S.D. 23.8 ± 3.4 yrs, 13 female), 22 middle-aged (31-55 yrs, 45.5 ± 7.9 yrs, 13 female) and 22 elderly participants (56-77 yrs, 64.7 ± 5.7 yrs, 13 female) participated in this study. All subjects had normal or corrected to normal visual acuity (20/20) and no visual field deficits as checked perimetrically. Exclusion criteria were a history of hemianopia, amblyopia, glaucoma, cataract, diplopia, nystagmus, cataract, Parkinson's disease, Alzheimer's disease and other disorders affecting the visual and oculomotor function. Written informed consent was obtained from all participants according to the Declaration of Helsinki (International Committee of Medical Journal Editors, 1991) after the institutional review board approved the study protocol.

3.2.2.   Experimental Protocol

Participants were instructed to maintain fixation at a fixation dot on a gamma corrected monitor (EIZO, CG241W, resolution of 2560×1440), which was placed at 67 cm distance. The white fixation dot (size: 10 pixels, luminance: 90 cd/m2) was presented against grey background (luminance: 29 cd/m2) in 40 trials lasting 7 sec each. The inter-stimulus interval was 3 sec, during which participants could rest their eyes. All participants were tested individually in a silent, dimly lit room.

3.2.3.   Eye movement recording

Binocular eye movements were recorded during the fixation task using an EyeLink-1000 system (SR Research, Ontario, Canada) with a sampling rate of 500 Hz and a spatial resolution of 0.01°. Head position was stabilized with a chin and forehead rest during eye tracker calibration, validation and recording.

3.2.4. **EEG recording**

During the fixation task, dense array EEG was simultaneously recorded with the eye movement data, using a HydroCell GSN 128-channel net and Net Amps 300 amplifier (EGI Inc., Eugene, Oregon, USA). Our recording used a sampling rate of 500 Hz, a 200 Hz anti-aliasing low pass filter, Cz as a reference (ground electrode between Cz and Pz), and was digitalized with 24-bit precision. Impedance was kept below 100 kΩ throughout the recording. Common trigger pulses were sent from the presentation computer to both eye tracking computer and EEG recording device for offline co-registration of eye movements and EEG.

3.2.5. **Data analysis**

3.2.5.1. Eye tracking and EEG data synchronization

Continuous EEG signal was re-referenced to the linked mastoids, filtered with high-pass (1 Hz) FIR filter, low pass (100 Hz) FIR filter, and notch (50 Hz) FIR filter. Eye tracking data and EEG data were synchronized and the synchronization quality was checked manually. Out-of-range eye tracking and EEG data were removed when there was a blink or when the eyes were not focused on the fixation point centered in a 4°x4° window.

3.2.5.2. Microsaccade detection

Microsaccade detection was performed based on the algorithm proposed by Engbert and colleagues (Engbert & Kliegl, 2003; Engbert & Mergenthaler, 2006). A microsaccade was defined by the following criteria: (i) the velocity exceeded six median-based standard deviations of the velocity distribution; (ii) the duration exceeds 12 msec; (iii) the inter-saccadic interval exceeded 50 msec, otherwise only the largest microsaccade would be kept. Then, binocular microsaccades were defined as those that occurred in left and right eyes with a temporal overlap. The criterion to confirm microsaccade detection validity was the main sequence relationship between

microsaccade amplitude and microsaccade velocity (Zuber et al., 1965). Microsaccade features include: rate (microsaccade number divided by detection time window length), amplitude (the Euclidean distance between the start and end point of the movement), velocity (the peak velocity during one microsaccade), duration, binocular microsaccade percentage (the proportion of binocular microsaccades in all detected microsaccades), horizontal and vertical binocular disconjugacy indices (Gao & Sabel, 2017).

3.2.5.3. Time frequency analysis

Binocular microsaccades and fixations were added as "events" into the EEG data. Epochs locked to binocular microsaccades [−0.5 s to 0.5 s] were extracted, baseline corrected [−0.2 s to 0 s], and manually screened for artifacts and noisy channels (on average 70.1 ± 85.1 epochs per subject discarded; 7.4 ± 5.2 channels per subject discarded and interpolated based on the activity of surrounding channels). On average, 117.9 ± 76.3 epochs in the young group, 147.1 ± 62.2 epochs in the middle-aged group, and 137.9 ± 82.5 epochs in the elderly group were analyzed. We quantified two typical microsaccade-related potentials, i.e. MLR and SP. Potential latencies were defined in grand averaged ERPs for each of the three groups. Within a short window around it (20ms for MLR; 10ms for SP), individual peak potential amplitude and latency were located. The time frequency decomposition analysis was performed on the EEG signals from 54 subjects. 12 subjects had to be excluded from analysis due to lack of eligible epochs (less than 50 epochs) in the recording so that this analysis was carried out only in 19 young, 17 middle-aged and 18 elderly subjects. The EEGLab function "newtimef" was used to compute ERSP and ITC across 25 linearly spaced frequencies ranging from 6 to 30 Hz and 200 linearly time points spanning -220 to 220ms around microsaccade onset. Representative electrodes were selected for the occipital region (E75, E70, E83), central region (E7, E31, E55, E80 and E106) and frontal region (E11, E19, E4) (Figure 2.1). We subdivided the time range into 8 small time windows (-220 to -150ms, -150 to -100ms, -100 to -50ms, -50 to 0ms, 0 to 50ms, 50 to 100ms, 100 to 150ms, 150 to 220ms), and the frequency range into 6 bands (alpha: 7-14 Hz, low alpha: 7-11 Hz, high alpha: 11-14 Hz, beta: 14-30 Hz, low beta: 14-18 Hz, and high beta: 18-

30 Hz).

3.2.5.4. Brain functional connectivity network analysis

Epochs locked to fixation onsets [0 s to 1s] were extracted to compare with epochs locked to microsaccade onsets, baseline corrected [0.3 s to 0.5 s], and manually screened for artifacts and noisy channels (on average 200.2 ± 95.1 epochs per subject discarded for fixation condition; 86.2 ± 62.7 epochs per subject discarded for microsaccade condition; 7.4 ± 5.2 channels per subject discarded and interpolated based on the activity of surrounding channels). Because microsaccade is a frequent eye movement that happens around once per second, not many pure fixation epochs as long as 1 s can be obtained. In order to get reliable results, we only performed brain functional connectivity analysis on the EEG signals from 19 subjects (9 females, 42.8 ± 18.2 yrs). On average, 93.6 ± 14.5 epochs per subject for fixation condition and 148.3 ± 6.2 epochs per subject for microsaccade condition were analyzed. Independent component analysis (ICA) was performed (Bell and Sejnowski, 1995). Each component was classified as either brain activity or artifacts e.g. eye blinks or muscle movement based on their topographic maps, power spectra, and temporal activity. On average 11.1 ± 2.0 components and 15.4 ± 5.3 components for microsaccade condition for microsaccade condition were back-projected into sensor space.

For source estimation, the forward model and the inverse model were calculated with software Brainstorm (Tadel et al., 2011). We calculated the forward model using the symmetric boundary element method (BEM) (Gramfort et al., 2010; Kybic et al., 2005) and default MNI MRI template (Colin 27). The inverse model was estimated using the weighted Minimum Norm Estimate (wMNE) (Hämäläinen & Ilmoniemi, 1994). When computing the inverse model (a) the source orientations were constrained to be normal to the cortical surface; (b) a depth weighting algorithm was used to compensate for any bias affecting the superficial sources calculation (Lin et al., 2006); and (c) a regularization parameter, $\lambda^2 = 0.1$ was used to minimize numerical instability, reduce the sensitivity of the wMNE to noise, and to effectively obtain a spatially

smoothed solution (Hämäläinen & Ilmoniemi, 1994). After estimating the activation time-courses at 15,002 vertices (an equilateral triangle in the tessellation of the cortical surface), 68 anatomical regions of interest (ROIs; 34 in each hemisphere) were generated based on the Desikan–Killiany atlas (Desikan et al., 2006) and activity of a seed voxel of each area was used to calculate functional connectivity.

Time frequency decomposition was conducted on source-based EEG single trials with Morlet wavelet (EEGlab newtimef function). The window size was set as 250 data points (500 ms). The wavelet contained 3 cycles at the lowest frequency (6 Hz) and the number of cycles was increasing up to 10 cycles at highest frequency (40 Hz) and 35 frequency points linearly spaced between 6 Hz and 40 Hz were estimated. After decomposition, for every subject, condition, and ROI, I obtained a 3D matrix of 35 (frequency points) × 200 (time points) × 'number of trials' (which varied between subjects). To evaluate the functional coupling, imaginary part of coherence (iCoh; Nolte et al., 2004) was computed for each frequency and time points between all possible pairs of ROIs. Number of trials used for iCoh calculation was kept the same between two conditions. iCoh is a conservative measure of functional coupling insensitive to volume conduction, which was calculated as,

$$iCoh_{(f,t)} = \left| Im \left(\frac{\sum_{n=1}^{N}(S_1^n(f,t)S_2^{n*}(f,t))}{\sqrt{\sum_{n=1}^{N}|S_1^n(f,t)|^2 \sum_{n=1}^{N}|S_2^n(f,t)|^2}} \right) \right| \qquad (3.1)$$

$S_1^n(f,t)$ and $S_2^n(f,t)$ are wavelet-decomposed EEG signals from ROI 1 and 2 respectively. * indicates the complex conjugate and |x| indicates the absolute value of x. For every subject (n=19), condition (2), and time- (200), and frequency point (35) we obtained a full 68 × 68 adjacency matrix of functional coupling.

To evaluate the microsaccade-related brain functional connectivity network characteristics, I converted these full iCoh adjacency matrices into sparse, undirected, weighted graphs, which can be further analyzed with graph measures. The functional coupling values above a certain threshold were retained and the values below this

threshold were set to 0. The threshold was adjusted for each full adjacency matrix to make sure the density of each graph (defined as the proportion of existing edges out of all possible edges) equals 0.20. In the weighted graphs, ROIs are the nodes and edges are the connections between different ROIs. Paths are the sequences of linked nodes that never visit a single node more than once. The global efficiency is the average inverse shortest path length in the network. The local efficiency is the global efficiency computed on node neighborhoods (Rubinov and Sporns, 2010). These two measures provide information of the communication efficiency in the brain. On a global scale, efficiency quantifies the exchange of information across the whole brain network, while the local efficiency quantifies a network's resistance to failure on a small scale.

3.2.6. Statistical analysis

ERSP and ITC values within different time windows, frequency bands, and locations were averaged separately for each subject and analyzed in group (3) × location (3) × frequency (6) × time (8) repeated-measures ANOVA. Due to the violation of sphericity assumption, Greenhouse-Geisser adjustion was applied to the degrees of freedom in the repeated-measures ANOVA. Bonferroni correction was applied to all post hoc tests and simple effect tests.

Global and local efficiency across 35 frequency points, 200 time points were compared between 2 conditions utilizing cluster-based permutation test. The number of randomization was set as 2000. The family-wise alpha level was set to 0.05. For each permutation, all t-scores corresponding to uncorrected p-values below the threshold of 0.05 were formed into clusters. The sum of the t-scores in each cluster is the "mass" (tmass) of that cluster. The most extreme cluster mass in each of the 2001 sets of tests was recorded and used to estimate the distribution of the null hypothesis.

3.2.7. Software

The experiment was developed in SR research Experiment Builder. Data analysis was conducted using Matlab 2016 and the following open-access toolboxes: EEGlab

(Delorme & Makeig, 2004), EYE-EEG extension (http://www2.hu-berlin.de/eyetracking-eeg) (Dimigen et al., 2011), Brainstorm (Tadel et al., 2011), and Brain Connectivity Toolbox (Rubinov & Sporns, 2010). Statistical analyses were performed using IBM SPSS Statistics 23 (IBM, USA, http://www.ibm.com/software/analytics/spss/).

3.3. Study II: Results

3.3.1. Microsaccade-related temporal-spectral power and synchronization dynamics

With respect to temporal-spectral power and synchronization dynamics, the overall group effect was not significant ($F(4,102) = 1.23$, $P = 0.304$, partial $Eta^2 = 0.05$). Figure 3.1 displays the ERSP and ITC change over time in different frequency bands over the occipital, central and frontal regions. There was a significant interaction between electrode location, time and frequency band in both ERSP and ITC ($F(11.4,583.7) = 4.41$, $P < 0.001$, partial $Eta^2 = 0.08$; $F(9.5,483.1) = 6.91$, $P < 0.001$, partial $Eta^2 = 0.12$). Simple effect analysis revealed the detailed temporal-spectral pattern after microsaccade onset: (i) alpha band ERSP increased and peaked within 100-150 ms in the occipital region (Figure 3.1 A, B) and ITC increased and peaked within 150-220 ms in all regions (Figure 3.1 C, D); (ii) beta band displayed no significant ERSP change in any region over time (Figure 3.1 A, B); (iii) low beta ITC increased and peaked within 150-220 ms in occipital and central regions, while in frontal region, it peaked within 0-50 ms; and (iv) high beta ITC increased and peaked within 0-50 ms in all regions (Figure 3.1 C, D) (all $P < 0.05$ after Bonferroni correction).
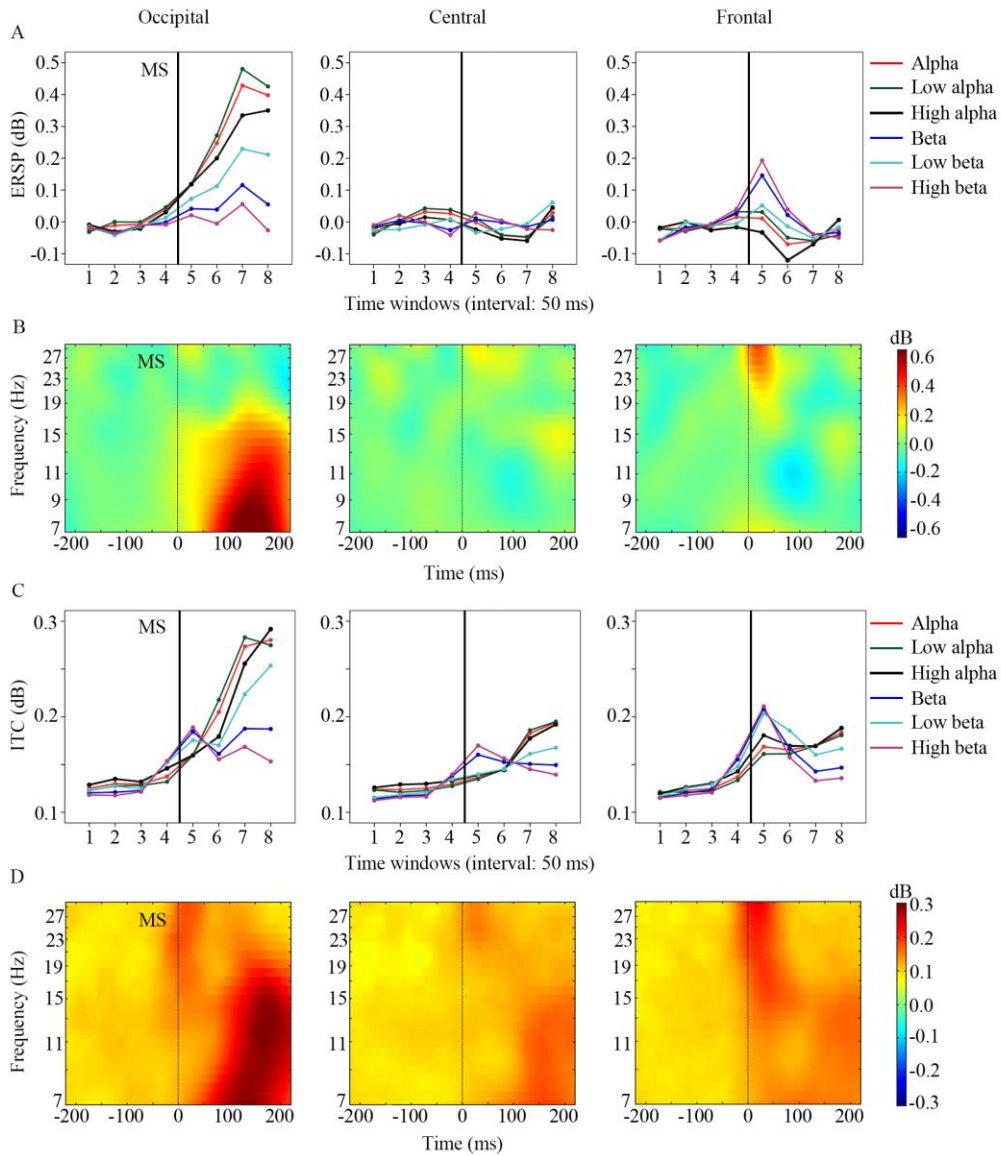
Figure 3.1. Event-related spectral perturbation (ERSP) and inter-trial coherence (ITC) changes

over time are displayed in different frequency bands over the occipital, central and frontal regions.

Panel A: ERSP change across 8 time windows in 6 frequency bands over the occipital, central and frontal regions. Panel B: ERSP change over time across 7-30 Hz frequencies over the occipital, central and frontal regions. Panel C: ITC change across 8 time windows in 6 frequency bands over the occipital, central and frontal regions. Panel D: ITC change over time across 7-30 Hz frequencies over the occipital, central and frontal regions. In panel A and C, time scales are: 1 = -220 to -150 ms; 2 = -150 to -100 ms; 3 = -100 to -50 ms; 4 = -50 to 0 ms; 5 = 0 to 50 ms; 6 = 50 to 100 ms; 7 = 100 to 150 ms; 8 = 150 to 220 ms. The vertical black lines represent microsaccade onset.

3.3.2. Microsaccade-related brain functional connectivity network dynamics

Cluster-based permutation tests revealed that, the local efficiency of the microsaccade-locked brain functional connectivity network was significantly higher than that of the fixation-locked network within alpha band from -200 ms to around 30 ms (tmass = 1049.3, P = 0.026) (Figure 3.2, upper row). The global efficiency of the microsaccade-locked network was significantly higher than that of the fixation-locked network within alpha band from -200 ms to around 160 ms (tmass = 1737.9, P = 0.010) (Figure 3.2, lower row).

Figure 3.2. Local and global efficiency dynamics of the microsaccade-locked and fixation-locked brain functional connectivity networks and the difference between the two networks. In the difference graphs (third column), the da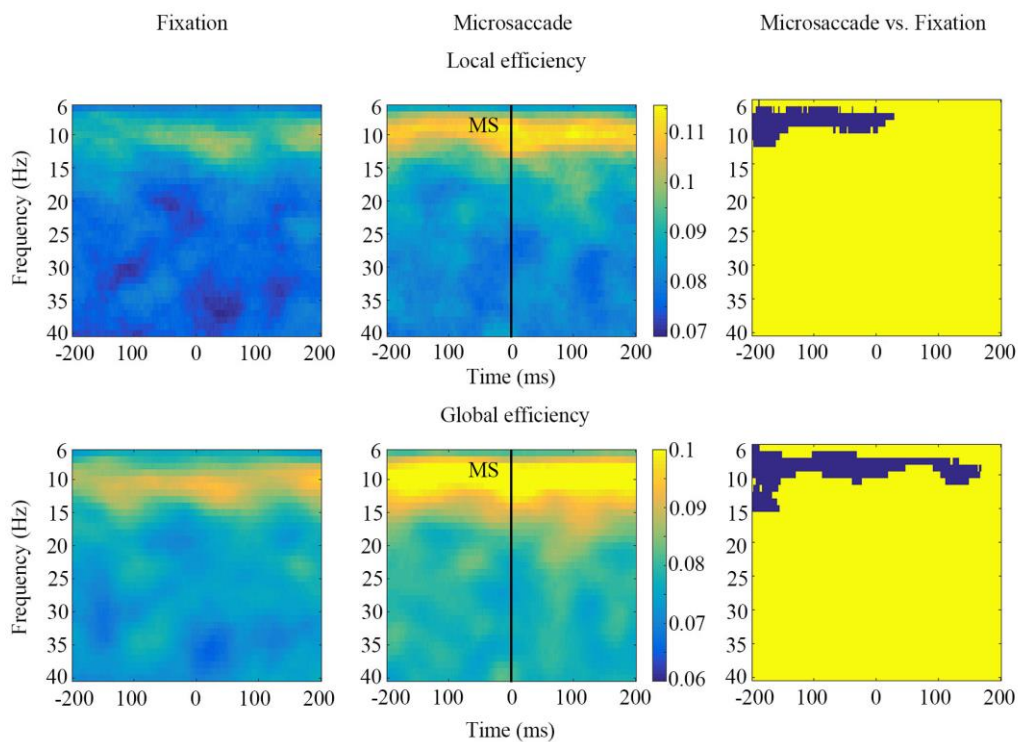rk blue indicates time-frequency regions significantly different between the microsaccade-locked and fixation-locked brain functional connectivity networks.

3.4.　Study II: Discussion

I report the first comprehensive assessment of microsaccade-related temporal-spectral power, synchronization dynamics, and brain functional connectivity network dynamics. This study uncovered that microsaccades can induce occipital alpha band perturbation and enhanced global alpha band cortical synchrony within the MLR time window. Local efficiency and global efficiency of the alpha-band functional network increased from 200 ms before microsaccade onset; and the increased global efficiency was maintained till around 160 ms after microsaccade execution. These results confirmed microsaccades' impact on brain activity and suggested a mechanism of cortical refreshment in addition to the retinal refreshment.

3.4.1.　Microsaccade-related temporal-spectral power and synchronization dynamics

Our temporal-spectral analysis captured characteristic oscillatory dynamic patterns after microsaccades in the alpha and beta frequency bands, and this dynamic pattern was maintained across the life span. Beta band spectral power was stable, but high beta ITC increased globally within the SP time window. The alpha band showed spectral perturbation locally in the occipital region and increased ITC globally within the MLR time window. These oscillatory dynamic patterns after microsaccades were observed during the time windows of both microsaccade-related potentials. We therefore need to consider two types of neuronal responses that contribute to ERP waveforms: the "evoked" type (phasic increase of postsynaptic activity in neuronal ensembles) and "phase reset" type (reorganization of the phase of ongoing neuronal oscillations) (Lakatos et al., 2009). It has been suggested that an increased ITC that accompanies oscillatory power enhancement is not considered to be a "phase reset" response but an "evoked" response　(Lakatos et al., 2009). To gain more insight into the mechanism underlying our finding of enhanced cortical synchrony, we compared the ERSP and ITC graphs (Figure 3.1). Within the SP time window, globally increased high beta ITC was not accompanied by increased ERSP, suggesting a "phase reset" function - perhaps induced by EMG signals, which accompanies microsaccade

execution. Within the MLR time window, enhanced alpha band cortical synchrony coincides with increased ERSP in the occipital region, suggesting the existence of an "evoked" response, while in the frontal and central regions, increased cortical synchrony existed without the presence of increased ERSP. This is an indication that "phase resetting" is taking place as well and is most visible outside the occipital region. Unlike intracortical electrode recording used in animal studies, which can probe neuron firing fluctuation and ongoing oscillation phase reset, with our EEG scalp recording we are unable to determine in the occipital region whether the enhanced cortical synchrony is a purely "evoked" response or a combined "evoked" and "phase reset" response, though we think that the latter is more likely. New studies are now needed to better understand the mechanism underlying such alpha band synchronization.

While our results experimentally confirmed previous observations by others of alpha resynchronization following MLR peak (Dimigen et al., 2009), we now present for the first time the alpha band power and synchronization dynamics underlying this phenomenon. Our findings suggest that microsaccades induced not only spectral perturbation locally in the occipital region, but they also reset alpha band phase globally, i.e. in frontal, parietal and occipital regions. We propose that such alpha-band synchronization play an important role in visual perception and, in a speculative spirit, they might function to help synchronize visual processing with other functional systems, which might relate to the "binding" problem (Singer, 1996). For example, as one theory of microsaccade function indicates, saccade-related corollary activity plays a crucial role in anticipatory preparation of visual centers for visual processing (Melloni et al., 2009). In fact, phase and amplitude of alpha activity are known to determine whether a stimuli reaches sensory awareness or not (Busch et al., 2009; Busch & VanRullen, 2010; Mathewson et al., 2009), and the saccade-induced phase is similar to the ongoing phase that leads to the maximal stimulus evoked response (Melloni et al., 2009). Thus, we propose the microsaccade-induced global alpha phase synchrony might facilitate the subsequent visual perception.

3.4.2.   **Microsaccade-related brain functional connectivity network dynamics**

Quantifying the brain functional connectivity network dynamics during microsaccades and fixations and comparing them revealed that both local and global efficiency of the brain network increased from 200 ms before the microaccade onsets. The increased local efficiency was maintained till around 30 ms after microsaccade, and the increased global efficiency was maintained till around 160 ms after microsaccades. These results revealed a characteristc brain functional connectivity network pattern related to microsaccades. Before microsaccade execution, the increased local and global efficiency within the alpha band network suggested enhanced communication between neighboring and remote brain regions (including visual cortex and multiple eye fields, Figure 1.11) during planning, coordination and preparation of the microsaccades. After microsaccade execution, the enhanced remote communication within alpha band was maintained till around 160 ms after microsaccades. We propose that this could also serve as a mechanism of microsaccades' function in cortical refreshment. Alpha-band large-scale network was proposed to play an attentional role, i.e. supporting active processing of task-relevant information and inhibiting task-irrelevant neuronal activity (Palva & Palva, 2011). By optimizing attention allocation, alpha band brain functional network is critical in determining what information gets the most processing resources, which in the next step influences higher cognitive functions utilizing the products of this visual processing. By enhancing remote communication efficiency in the brain, microsaccades facilitate the coordination of this attention system.

3.5.   Study II: Conclusion

Microsaccades induced occipital alpha band perturbation and enhanced global alpha band cortical synchrony within the MLR time window. Local efficiency and

global efficiency of the alpha-band functional network increased from 200 ms before microsaccade onset; and the increased global efficiency was maintained till around 160 ms after microsaccade execution. In sum, I propose that microsaccades play a significant role in vision not only through retinal image refreshing (Engbert & Mergenthaler, 2006), which counteracts visual fading, but also through "cortical refreshment", i.e. resetting alpha band phase globally and increasing the global efficiency of the brain functional connectivity network to prepare (sensitize) the brain for subsequent visual processing. Future studies should further clarify the mechanisms of "cortical refreshment" to uncover their contribution in visual processing and its relationship with other non-visual functions in normal and abnormal vision.

4. Study III: Microsaccade dysfunction and adaptation in hemianopia after stroke

Published in:

4.1.   Study III: Introduction

4.1.1.   Unexplained visual symptoms in hemianopia after stroke

One cause of vision loss is brain stroke or trauma, leading to homonymous hemianopia (Rowe et al., 2009; Sand et al., 2013). While visual field defects in hemianopia can be well characterized with perimetry, visual field size and topography correlate poorly with vision-related quality of life (Gall et al., 2010; Gall et al., 2009; Gall et al., 2008; Papageorgiou et al., 2007). Besides the reduction of visual field size, patients may also experience other still poorly understood symptoms such as blurred vision, diplopia, or reduced visual acuity (G. A. de Haan et al., 2015; Poggel et al., 2007; Rowe et al., 2013). And there are even deficits in the "intact" field ("sightblindness") (Bola et al., 2013a, 2013b).

4.1.2.   Microsaccade is one potential contributor to these visual impairments

One important contributor to these visual impairments may be microsaccades, a key element in normal vision (Martinez-Conde et al., 2013). The reasons why we suspected microsaccade alterations in hemianopia are two-fold: (i) altered microsaccades can cause blurred (foggy) vision and low visual acuity (Ciuffreda & Tannen, 1995; Foroozan & Brodsky, 2004), which were reported in hemianopia (Rowe et al., 2013); (ii) microsaccades are controlled by a complex brain functional

connectivity network involving the superior colliculus (SC) (Hafed et al., 2009), multiple eye fields, and visual cortex (Lynch, 2009). Given that brain network disturbances are responsible for functional impairments well beyond the local lesion (Catani et al., 2012), possible connectivity alteration between the damaged visual system and cortical eye fields is to be expected in hemianopia. Examples of network disturbances in vision loss are especially the occipital-frontal functional connectivity (Bola et al., 2014; Bola et al., 2015; A. R. Carter et al., 2012; Fallani et al., 2007; Grefkes et al., 2008), which synchronizes visual cortex with frontal eye fields. Therefore, to better understand vision loss in hemianopia, the functional status of microsaccades and their binocular conjugacy needs clarification.

4.1.3. Study aim and hypotheses

In this case-control study, we compared microsaccade features in hemianopia to those in healthy controls and correlated them with visual performances and lesion age. Based on prior reports, we expected three altered microsaccade features in hemianopia: (i) enlarged microsaccade amplitude due to a decreased inhibition of the SC after visual deafferentation (Shi et al., 2012); (ii) reduced binocular microsaccade conjugacy due to miscalibration of the eye movement control network after visual input deprivation (Schneider et al., 2013); and (iii) microsaccade direction bias towards the deficit side, which was reported in hemianopia (Reinhard et al., 2014).

4.2.   Study III: Methods

4.2.1.   Participants

For this case-control study 14 patients with homonymous hemianopia including incomplete hemianopia (13 male /1 female; mean age: 59, range from 45 to 73) and 14 healthy controls (11 male / 3 female; mean age: 60, range from 44 to 71) were recruited and tested from February 2014 to September 2015. Both groups did not differ in age ($t(26) = -0.13$, $P = 0.897$). Table 4.1 shows the patients' demographic and medical characteristics.

Table 4.1. Patients' demographic and medical characteristics

Patient	Age (year)	Gender	Lesion age (month)	Cause of damage	Visual field defect
01	45	male	61	Left PCA infarct	right upper quadrantanopia
02	65	male	20	Left PCA infarct	right lower quadrantanopia
03	68	male	45	Right OL ischemia	left hemianopia
04	73	male	19	Left PCA infarct	right hemianopia
05	62	male	28	Left PCA infarct	right hemianopia
06	52	male	29	Right PCA infarct	left upper quadrantanopia
07	49	male	11	Right PCA infarct	left hemianopia
08	66	male	49	Right PCA infarct	left hemianopia
09	72	male	19	Right OL stroke	left lower quadrantanopia
10	45	male	43	Right PCA infarct	left hemianopia
11	53	male	93	Left OL stroke	right hemianopia
12	58	male	6	Left OL infarct	right hemianopia and left upper quadrantanopia
13	61	male	6	Right PCA and PICA infarct	left hemianopia
14	60	female	7	Right PCA infarct	left lower quadrantanopia

Abbreviations: PCA = posterior cerebral artery; OL = occipital lobe; PICA = posterior inferior cerebellar artery

Inclusion criteria: hemianopia after posterior artery stroke-related occipital cortex damage with lesion age $\geq$ 6 months. Exclusion criteria: complete blindness, visual hemi-neglect, psychiatric diseases (schizophrenia etc.), serious substance abuse, diabetic retinopathy or diabetes mellitus with average blood glucose level above 7mmol/l, blood pressure instable and > 160/100mmHg, instable or high level of intraocular pressure (> 27mm of hg column), retinitis pigmentosa, pathological nystagmus, and any ophthalmological disorder affecting visual functions.

All subjects gave written informed consent to participate in the study according to the Declaration of Helsinki (International Committee of Medical Journal Editors, 1991) and the institutional review board approved the study protocol.

4.2.2. Experimental protocol

Participants were instructed to maintain fixation at a fixation dot on a gamma corrected monitor (EIZO, CG241W, resolution of 2560×1440), which was placed at 67 cm distance. The white fixation dot (size: 10 pixels, luminance: 90 cd/m2) was presented against grey background (luminance: 29 cd/m2) in 40 trials lasting 7 sec each. The inter-stimulus interval was 3 sec, during which participants could rest their eyes. All participants were tested individually in a silent, dimly lit room.

4.2.3. Eye movement recording

Binocular eye movements were recorded during the fixation task using an EyeLink-1000 system (SR Research, Ontario, Canada) with a sampling rate of 500 Hz and a spatial resolution of 0.01°. Head position was stabilized with a chin and forehead rest during eye tracker calibration, validation and recording.

4.2.4. Visual performances

Visual acuity was measured with the standard Landolt 'C' test at a 40 cm distance (Standard-Snellen, with see-chart from Oculus), contrast sensitivity with the MARS contrast chart (MARS Perceptrix Corporation), dynamic vision performance with

Düsseldorf Dynamic Vision Test, and visual fields parameters with a high-resolution computer-based campimetric visual field test with super-threshold stimuli (HRP; Figure 4.1) (Sabel et al., 2004). For HRP, we analyzed the size of blind areas and ARVs in the whole visual field (covering 25°x25° of subjects' visual field), response time in the whole visual field, in intact areas and in ARVs. Figure 4.1 illustrates how we define the central 10° by 10° region, blind areas, ARVs and intact areas.
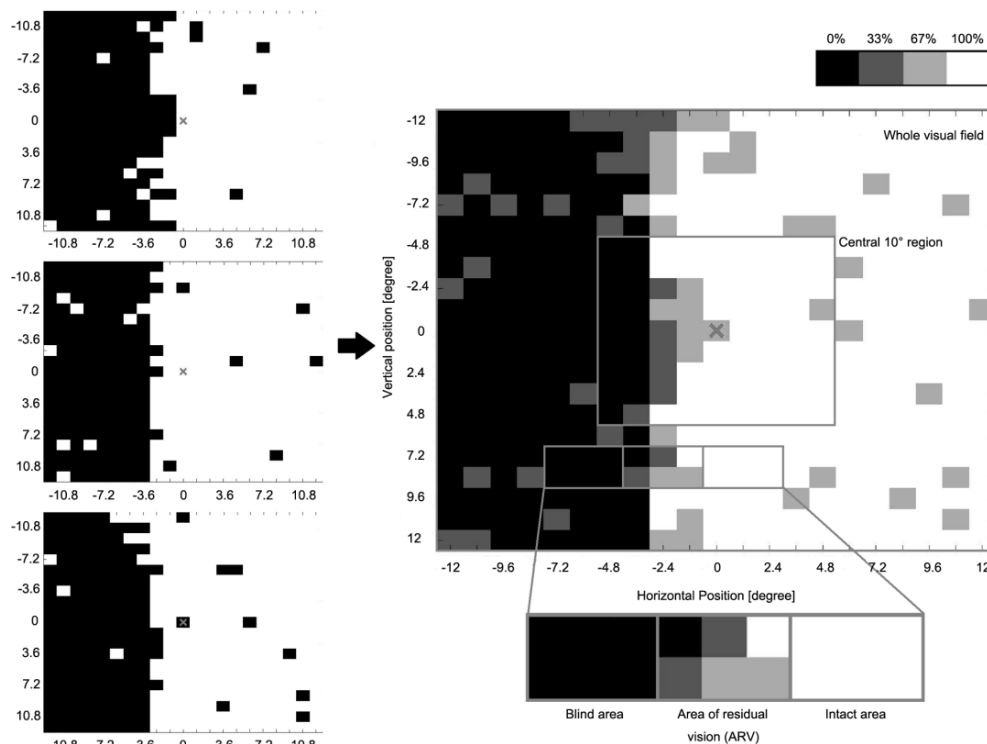
Figure 4.1. Visual area categorization based on visual field chart from high-resolution computer-based perimetry (HRP). During HRP, a supra-threshold stimulus detection task was carried out three times, creating three simple detection charts (left column). The white area shows the intact visual field, while the black area shows blind regions. By superimposing these three detection charts, we obtained a new visual chart (right center). The emerging grey area represents visual field sectors where patients' response accuracy was inconsistent; with light grey representing the area where patients responded to 2 / 3 targets and dark grey represents areas with 1/3 response. All grey areas together are defined as "areas of residual vision" (ARVs). The black areas and the white areas were defined as being blind or intact, respectively. We also analyzed the central square region 10° by 10°.

4.2.5. **Eye movement data analysis**

4.2.5.1. Microsaccade detection

Microsaccade detection was based on published algorithms (Engbert & Kliegl, 2003; Engbert & Mergenthaler, 2006) and programmed in Matlab (Mathworks, Massachusetts, U.S.A). The time series of eye positions were transformed to velocities by calculating a moving average of velocities over five data samples. A microsaccade was defined by the following criteria: (i) the velocity exceeded six median-based standard deviations of the velocity distribution; (ii) the duration exceeds 12 msec (6 data samples); (iii) the inter-saccadic interval exceeded 24 msec (12 data samples). The criterion to confirm microsaccade detection validity was the main sequence relationship between microsaccade amplitude and microsaccade velocity (Zuber et al., 1965). Microsaccade features we analyzed were rate (microsaccade number devided by detection time window length), amplitude (the Euclidean distance between the start and end point of the movement), velocity (the peak velocity during one microsaccade) and duration.

4.2.5.2. Conjugacy analysis

Binocular microsaccades were defined as those that occurred in left and right eyes with a temporal overlap as defined by Engbert and Kliegl (Engbert & Kliegl, 2003). After detection of these binocular microsaccades, binocular microsaccade percentage was calculated as the proportion of binocular microsaccades in all detected microsaccades.

We paired the microsaccades from the two eyes in each overlapped time window and resolved each microsaccade into one horizontal component x and one vertical component y. For each pair of eyes we defined two components for the left (xl and yl) and right eye (xr and yr) to calculate the disconjugacy indices using the following equations:

$$\text{Horizontal disconjugacy index (dCX)} = |xl - xr| \quad (4.1)$$

$$\text{Vertical disconjugacy index (dCY)} = |yl - yr| (4.2)$$
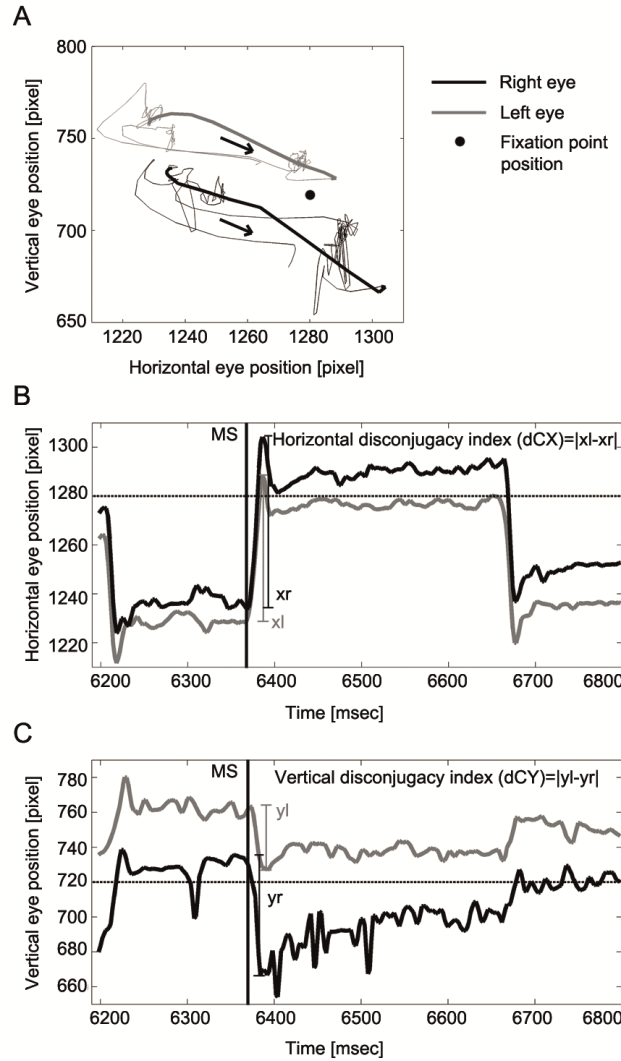
Figure 4.2. Trajectory (A), horizontal (B) and vertical (C) binocular disconjugacy indices of one microsaccade. Panel A presents the trajectory of one microsaccade (bold lines). The black arrows indicate the moving direction of the microsaccade. Panels B and C illustrate the calculation of horizontal (dCX) and vertical disconjugacy index (dCY) for this pair of binocular microsaccades. Left and right eye movements are represented by grey or black solid lines, respectively; the fixation point position is represented by the horizontal dotted lines (in B and C) or black dot (in A). Black solid vertical lines (in B and C) indicate the onset of one microsaccade (around 6360 ms). Larger values of dCX and dCY indicate larger discrepancies between two eyes, i.e. poorer binocular conjugacy.

Larger values of these two indices represent larger discrepancy between the two eyes, indicating poorer binocular conjugacy (Figure 4.2). Thus, we obtained binocular microsaccade percentage, dCX and dCY for each subject.

4.2.5.3. Classifying microsaccades based on their direction

In the hemianopia group, monocular and binocular microsaccades were classified as belonging to one of two categories according to their direction: bias towards the deficit or bias towards the intact hemifield. This direction bias was calculated as follows:

$$Microsaccade\ direction\ bias = \frac{\text{numbers of microsaccades towards the deficit hemifield}}{\text{number of microsaccades towards the intact hemifield}}$$

(4.3)

Patients with no bias towards either hemifield had a microsaccade direction bias equal to 1. Values >1 represent bias towards the deficit hemifield and values <1 represent bias towards the intact hemifield.

In incomplete hemianopia, when patients show no bias towards either field, microsaccade direction bias is susceptible to the area ratio of the deficit and intact areas. For convenience of inter-subject comparison, we calculated the microsaccade direction bias in incomplete hemianopia as follows:

$$MS\ direction\ bias = \frac{\text{numbers of microsaccades towards the deficit area}}{\text{number of microsaccades towards the intact area}} \times \frac{\text{intact area size}}{\text{deficit area size}}$$

(4.4)

After this correction, microsaccade direction bias also equals 1 when patients with incomplete hemianopia show no direction bias.

4.2.6. **Statistical analysis**

Independent-sample t tests were conducted to test the microsaccade feature differences between the heminopia group and the control group. Before conducting between-groups statistical tests, normality of distribution was assessed with Shapiro-Wilk test. For measures violating the normal distribution assumption, Mann-Whitney U test was used. One-sample t tests were performed to test the microsaccade direction bias against 1. A criterion of $P = 0.05$ (two-tailed) was set for all statistical tests. Bonferroni-Holm correction was performed to correct for multiple comparisons and are reported as Pcor. As this is the first explorative study on microsaccades in hemianopia, we also present the original p values and discussed the results as a reference for future studies.

Pearson's correlations were calculated between patients' microsaccade features (binocular microsaccade percentage, dCX, dCY, microsaccade rate, amplitude, velocity, duration, monocular and binocular microsaccade direction bias), lesion age, and visual performances (visual acuity, contrast sensitivity, dynamic vision performance, fixation accuracy during HRP, blind area and ARVs sizes in the whole visual field and central 10 ° region, mean response time in the intact visual field and ARVs). A bootstrapping method was utilized to reduce spurious findings (5000 samples, bias-corrected and accelerated 95% confidence interval).

Statistical analyses were performed using IBM SPSS Statistics 22 (IBM, USA, http:// www.ibm.com/software/analytics/spss/) and R-Studio (version 0.99.903, RStudio Team, USA, http://www.rstudio.com).

4.3.   Study III: Results

None of the participants dropped out from the study. After microsaccade detection and computation of microsaccade features, main sequences were generated for all microsaccades in both groups (Figure 4.3).
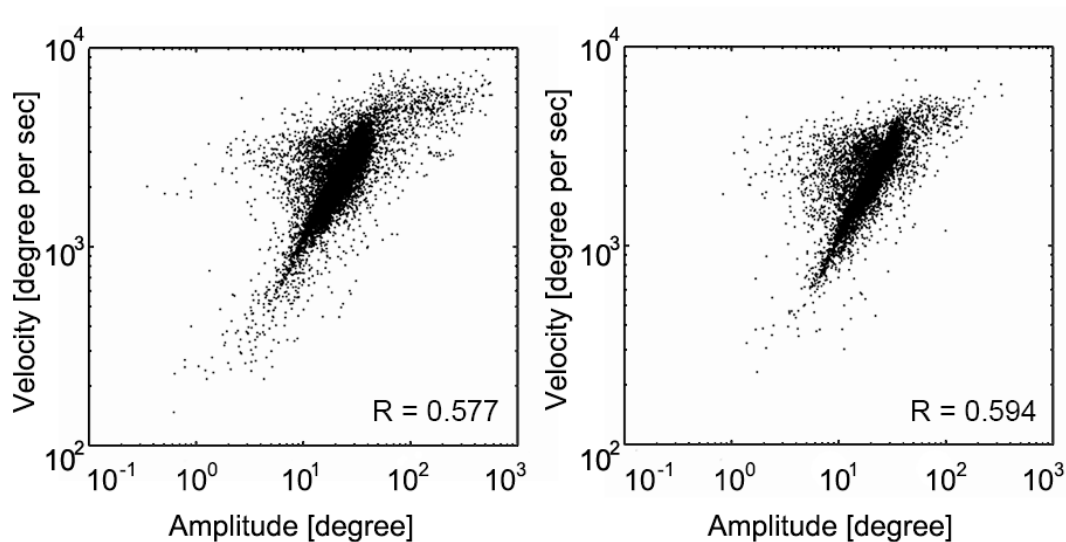
Figure 4.3. Microsaccades main sequence. Main sequence for all microsaccades in the hemianopia (left) and control group (right). The humps toward the left in both groups' main sequence graphs are due to the slope variance in subjects. The correlation coefficient R values are displayed for each group.

4.3.1.   Comparison between hemianopic patients and normal controls

Table 4.2 presents the summary of all microsaccade features and the statistics of the group differences. Consistent with our hypotheses, the hemianopia group displayed larger microsaccade amplitude and reduced horizontal and vertical binocular conjugacy. Hemianopic patients also exhibited longer microsaccade duration. The group difference in horizontal disconjugacy was significant even when Bonferroni-Holm correction was applied. No group difference was discovered in other microsaccade features such as rate, velocity, and binocular microsaccade percentage.

To rule out the possibility that such binocular disconjugacy was due to the differences in eye tracker calibration, we compared the binocular difference in calibration outcomes of the hemianopia and control groups with an independent sample two-tailed t test and found them to be comparable (hemianopia: mean = 0.14 deg, SEM = 0.06 deg; controls: mean = 0.06 deg, SEM = 0.01 deg; $t(14.22) = 1.25$, $P = 0.230$). Figure 4.4 displays examples of the binocular conjugacy patterns of one patient and one control subject.

4.3.2. Microsaccade direction bias in hemianopia

One-sample t-test results showed that the hemianopia group's monocular (mean = 0.89, SEM = 0.11) and binocular microsaccade direction bias (mean = 1.03, SEM = 0.24) were not significantly different from 1 ($t(13) = -1.07$, $P = 0.304$; $t(13) = 0.13$, $P = 0.898$).

Further examination of patients' individual microsaccade distribution revealed that 7 of 14 patients showed a microsaccade direction bias towards the intact areas whereas the other seven did not have any bias. To explore the difference between these two kinds of responses, we subdivided the hemianopia group into two subgroups: a biased and a non-biased group. Figure 4.5 illustrates their respective monocular and binocular microsaccade direction bias.

Table 4.2. Microsaccade features in hemianopia and control groups and the group differences

Microsaccade features	Hemianopic group (n = 14)	Control group (n = 14)	t	P	P_{cor}	95% confidence interval
Amplitude (degree)	0.46 ± 0.03	0.38 ± 0.02	2.34	0.027	0.162	-0.009, 0.144
Horizontal disconjugacy (min arc)	10.39 (20.59)[a]	8.01 (4.39)[a]	31.00[b]	0.002	0.014	n/a
Vertical disconjugacy (min arc)	9.62 (30.24)[a]	7.57 (7.98)[a]	52.00[b]	0.035	0.175	n/a
Binocular microsaccade percentage (%)	0.48 ± 0.06	0.55 ± 0.04	-0.98	0.336	0.744	-0.205, 0.072
Microsaccade rate (num per sec)	1.41 ± 0.23	1.37 ± 0.20	0.13	0.894	0.894	-0.581, 0.663
velocity (degree per sec)	43.21 ± 1.44	41.05 ± 1.12	1.18	0.248	0.744	-1.589, 5.894
Duration (msec)	17.64 ± 0.92	15.42 ± 0.44	2.18	0.042	0.175	0.086, 4.349

[a] Normal distributed microsaccade feature values are displayed as mean ± SEM, while non-normal distributed feature values are displayed as median (range).

[b] Mann-Whitney U tests were performed and U values are presented here because the data was not normally distribute
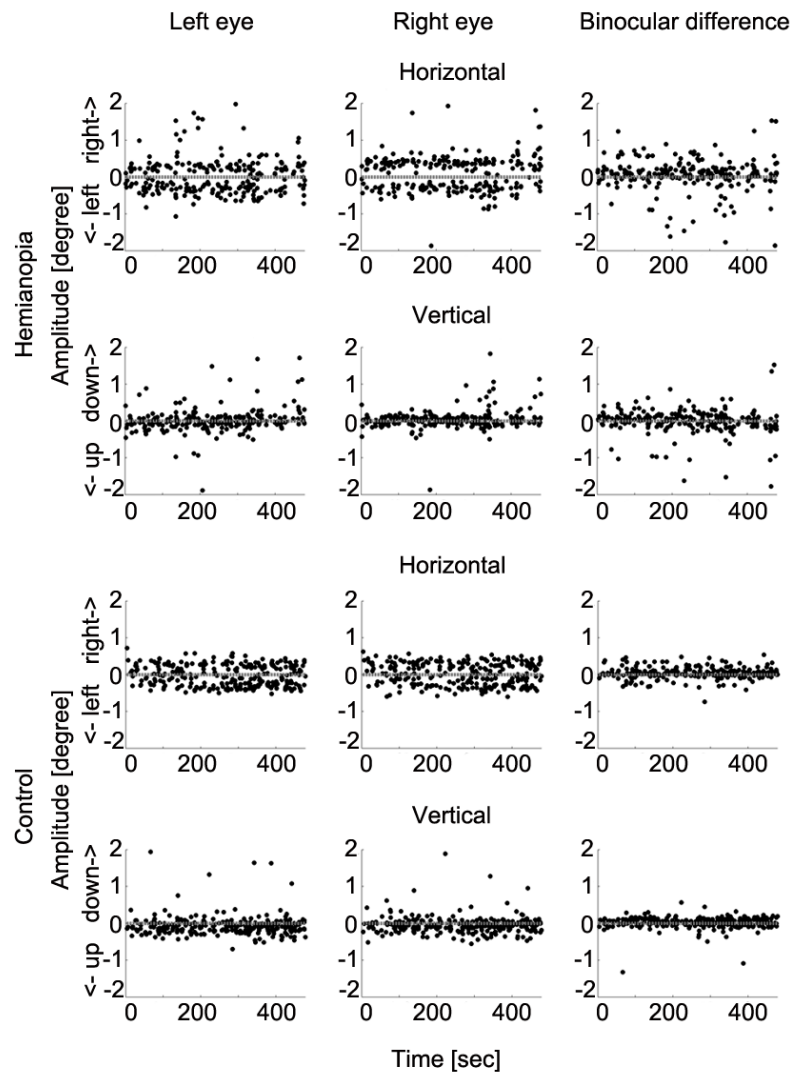
Figure 4.4. Microsaccade binocular conjugacy patterns in one hemianopic patient and one control subject. *The upper two rows show the horizontal and vertical microsaccade components of one participant with hemianopia and the binocular difference. The lower two rows display the same for one control subject. Each dot represents one microsaccade. The horizontal dotted lines represent the fixation point position. The hemianopic patient shows larger binocular difference, both in the horizontal and vertical directions.*
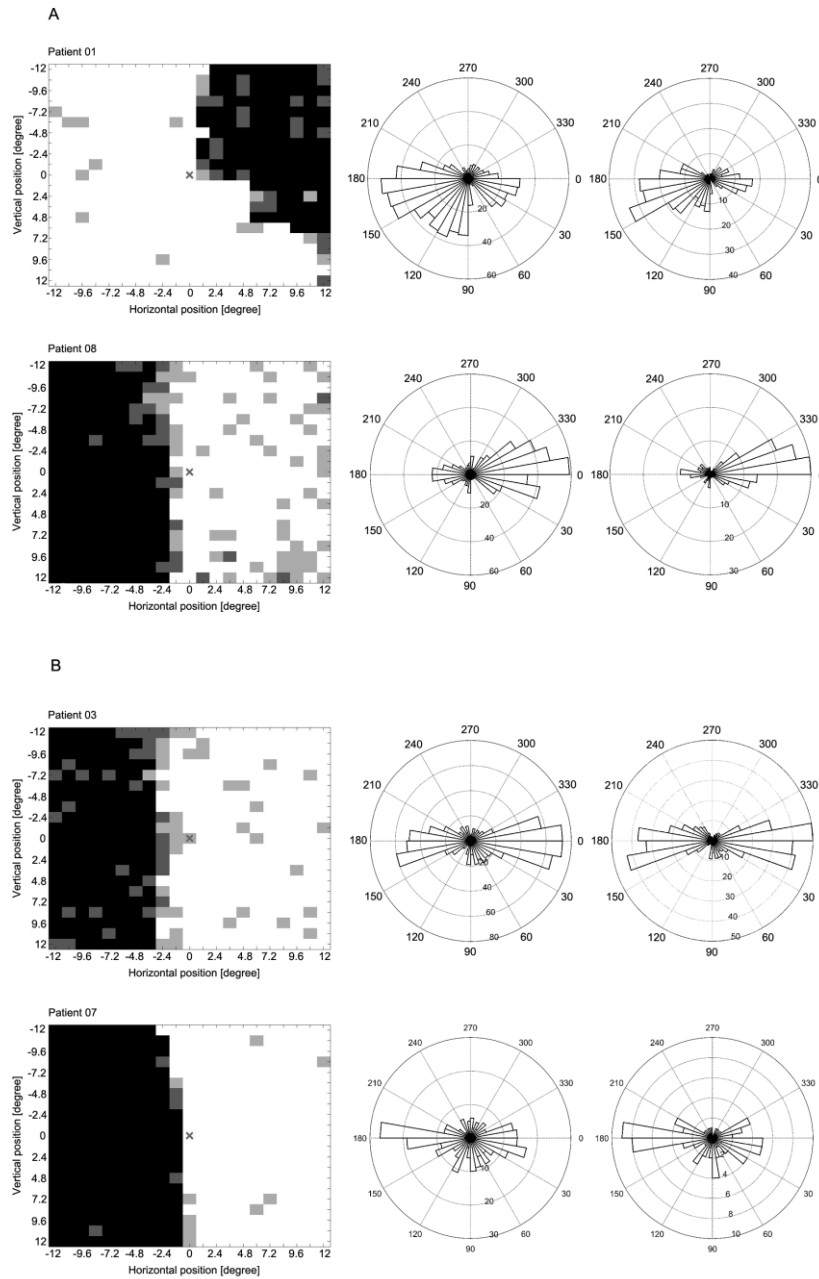
Figure 4.5. HRP visual charts, monocular and binocular microsaccade angular histograms of representative hemianopia cases of the biased (A) and the non-biased group (B). The HRP visual charts (first column) and angular histograms of monocular (second column) and binocular (third column) microsaccades from four patients with hemianopia (two in each subgroup) are presented. In the biased group, the angular histograms show more microsaccades towards the intact area. In the non-biased group, the angular histograms show no specific bias of microsaccade direction towards the blind or intact areas. Note: The angular histograms do not convey information about microsaccade amplitudes. Bar length rather represents microsaccade numbers.

To confirm that our selection led to distinct subgroups, we tested their microsaccade direction bias against 1. The results confirmed that both monocular and binocular microsaccades were towards the intact area in the biased group (monocular: mean = 0.66, SEM = 0.06, t(6) = -5.41, p = 0.002; binocular: mean = 0.41, SEM = 0.08, t(6) = -7.45, p < 0.001) while the non-biased group showed no specific bias (monocular: mean = 1.12, SEM = 0.16, t(6) = 0.73, p = 0.494; binocular: mean = 1.66, SEM = 0.33, t(6) = 2.02, p = 0.090).

Next we tested the subgroup differences in all microsaccade features, lesion age, visual field defect parameters and visual performances. The two subgroups differed in reaction time in ARVs: the biased group (mean = 0.50 sec, SEM = 0.02 sec) responded significantly faster to the visual stimuli than the non-biased group (mean = 0.56 sec, SEM = 0.03 sec; t(12) = -2.28, p = 0.042, pcor = 0.456). This difference did not reach the significance level after Bonferroni-Holm correction and interpretation of these should therefore be considered as preliminary.

Considering the fact that only half of the hemianopia group displayed a microsaccade direction biased towards the intact area, one possibility exists that such a bias is a function of the residual vision on the hemianopic side, i.e. a larger seeing area on the deficit side would lead to a more balanced distribution of microsaccades towards the two visual hemifields resulting in a smaller microsaccade direction bias value. But a Pearson's correlation analysis revealed no such relationship between microsaccade direction bias and the size of the seeing areas on the hemianopic side (r(14) = 0.19, P = 0.512, bootstrapped CI_95 = -0.42 to 0.67) and no difference was observed regarding the size of the seeing areas between the two subgroups (t(12) = -0.62, p = 0.546). Thus, the size of the seeing area on the hemianopic side does not explain the development of the microsaccade direction bias. Another possibility is that the microsaccade direction bias was caused by their tendency to produce microsaccades toward one direction, i.e. towards the right or the left. But checking the influence of the hemianopic side of the biased group revealed that 3 patients were left hemianopic and 4 patients were right hemianopic, which does not support this possibility.

4.3.3. Correlations between microsaccade features, lesion age and pathological parameters

Lesion age was found to be positively correlated with dCX ($r(14) = 0.67$, $P = 0.009$, bootstrapped CI_95 = 0.09 to 0.88), dCY ($r(14) = 0.75$, $P = 0.002$, bootstrapped CI_95 = 0.12 to 0.92) and microsaccade amplitude ($r(14) = 0.55$, $P = 0.043$, bootstrapped CI_95 = 0.12 to 0.87). Visual acuity was positively correlated with binocular microsaccade percentage ($r(14) = 0.59$, $P = 0.027$, bootstrapped CI_95 = 0.09 to 0.86), and negatively correlated with microsaccade velocity ($r(14) = -0.66$, $P = 0.011$, bootstrapped CI_95 = -0.89 to -0.22).

4.4. Study III: Discussion

We report the first comprehensive assessment of microsaccade features in patients with homonymous hemianopia and their relation with lesion age, visual field defect topography and visual performances. We found microsaccades to be enlarged in amplitude, prolonged in duration and impaired in their binocular conjugacy. These alterations were more severe in patients with older lesions, suggesting that these alterations are the consequence of the enduring experience of the vision loss, rather than a direct consequence of the brain damage and the associated acute visual field loss. Yet, microsaccade velocity was not significantly different from that of control subjects, indicating that motor aspects of eye movement generation were preserved after our patients had their posterior artery stroke damage (Shakespeare et al., 2015). Hemianopic patients did not show a microsaccade direction bias towards the deficit area as we hypothesized. Interestingly, half of our patients showed a microsaccade direction bias towards the seeing field and exhibited faster stimulus detection in ARVs. In addition, patients with a greater number of binocular microsaccades and slower microsaccade velocity performed better in visual acuity tests.

4.4.1. Microsaccade enlargement

We found microsaccade enlargement in combination with prolonged microsaccade duration and interpret this to indicate decreased inhibition of the SC after the cortical damage. The microsaccade control network is known to involve the SC and downstream nuclei (Hafed et al., 2009) and it receives visual input from different cortical regions that, aligned with the retino-collicular map (Triplett et al., 2009), which can modulate the excitation-inhibition balance in the SC (Populin, 2005). Visual input deprivation can cause insufficient inhibition of the SC, resulting in microsaccade enlargement in amblyopia (Shi et al., 2012) and PSP (Otero-Millan et al., 2011a). In hemianopia, visual field defects deprive the SC of visual input, which may cause insufficient inhibition by the SC, resulting in microsaccade enlargement and prolongation.

4.4.2. **Binocular disconjugacy**

We also discovered that the microsaccade binocular conjugacy was impaired in hemianopia. Such impaired binocular conjugacy was also described in monocular vision loss by Schneider et al. (Schneider et al., 2013) who proposed that visual inputs play a significant role in optimizing the eye movement network performance and that deprivation of it will disturb the calibration of this eye movement control network. This hypothesis is supported by the lesion-age dependency of microsaccade alterations we found: it suggests that the extended time of visual deprivation is a critical factor in the chronic phase of stroke, i.e. the longer the visual deficit lasts, the greater the disturbance of calibration reference and coordination within the brain functional connectivity network. As time passes, the eye movement control network then becomes gradually more uncoordinated, like an airplane going slightly off course for a short time will have a smaller impact on its displacement than when this deviation lasts longer.

In addition, it is conceivable that the brain functional connectivity network disturbance that develops after brain damage may also affect eye movement control. Bola et al. (2014) reported a loss of occipito-frontal functional connectivity in patients with optic nerve damage (Bola et al., 2014). The status of the functional connectivity

between occipital and frontal areas is of great relevance to communication between the frontal eye field and visual cortex. But how the brain functional connectivity network between eye fields and visual cortex is disturbed in hemianopia and how this disturbance influences eye movements needs to be clarified in future studies.

4.4.3. **Microsaccade alterations and visual performance**

Finally, we correlated microsaccade features and visual performance and found that microsaccades and their binocular conjugacy help explain the visual impairments in hemianopia. Patients' binocular microsaccade percentage correlated positively with their visual acuity. Furthermore, smaller microsaccade velocity was associated with better visual acuity. This supports the significant role of binocular microsaccades in high resolution vision and their role of preventing fading (Martinez-Conde, 2006) and correcting binocular disparity (Engbert & Kliegl, 2004). We speculate that too fast microsaccades might cause unstable and blurred vision, reducing visual acuity.

4.4.4. **Microsaccade direction: towards the intact or the deficit area?**

Reinhard et al. reporeted more fixational eye movements towards the deficit area in hemianopia (Reinhard et al., 2014). This is similar to the well-known strategy for macrosaccades in hemianopic patients after several months post trauma (Bahnemann et al., 2014; Meienberg et al., 1981; Pambakian et al., 2000) or after saccade training (Kommerell et al., 1999; Nelles et al., 2001). However, our results regarding microsaccades revealed the opposite: half of the hemianopia group showed a microsaccade direction bias towards the intact area, while the other half showed no direction bias.

In contrast to Reinhard´s study (Reinhard et al., 2014), which includes microsaccades, tremors and drifts, in our study we specifically focused on the distribution of the microsaccades only. One source of the discrepancy between both studies may be a difference between microsaccade direction and drift direction. In our 14 patients, we observed two microsaccade distribution patterns, a biased and a non-

biased one. We applied post hoc tests to explore the subgroup difference in visual field defect parameters and visual functional performance, and found that the biased group detected visual stimuli faster in ARVs compared to the non-biased group. Although this difference did not survive the multiple comparison correction, it may guide us to generate a new hypothesis. Because microsaccade direction bias has already been suggested to reflect increased attention (Engbert, 2006; Engbert & Kliegl, 2003; Otero-Millan et al., 2008; Pastukhov et al., 2013), we hypothesize that a microsaccade direction bias in about half of the hemianopic patients is a sign of a greater allocation of attention towards their seeing field (including ARVs). Such an adaptive attention allocation in the ARVs may be the cause why such patients had faster reaction times in ARVs.

In any event, in the intact area of the visual field the bottom-up activation by visual stimulus presentation is sufficient for the visual signals to reach the perceptual threshold. In ARVs, however, the relative defects caused by diffuse cell loss or cell inactivity supports only inconsistent response accuracies (Sabel et al., 2011). But whether or not the visual stimulus in ARVs reaches the perceptual threshold depends on the activity state of the partial (bottom-up) visual input and a sufficient (top-down) influence of attention. Because both acute and chronic attention allocation to the ARVs improves stimulus detection (Poggel et al., 2006; Poggel et al., 2004), and because microsaccade biases are linked to attention, we propose that the microsaccade direction bias towards the seeing field in hemianopia is adaptive for visual field deficits and may support vision recovery and restoration.

In sum, we uncovered a microsaccade pattern that is different from that of macrosaccades and may be due to their different functions in normal vision. Whereas in hemianopia macrosaccades (1-30 degrees of visual angle) are used to move objects located in the deficit area into to the intact visual field, microsaccades are very small (up to 1 degree) and their function is rather to refresh vision, prevent fading, and serve as a sampling tool in a relative small and more local region of the visual field. We propose that whereas macrosaccades help to capture visual scenes on the deficit side in

hemianopia, microsaccades are adaptive for visual perception itself and thus improve acuity and visual performance in the intact and in the partially damaged visual field. But further studies are needed to clarify the visual functions and performance differences between patients with different microsaccade patterns to be able to determine which elements are maladaptive and which are adaptive for vision.

4.5.   Study III: Conclusion

Overall, we propose that microsaccade alterations in hemianopia are both good and bad news. On one hand, microsaccade enlargement and impaired binocular conjugacy suggest malfunctioning microsaccade control circuits due to visual deprivation and disturbed brain functional connectivity network. On the other hand, among hemianopic patients, those who give up their normal microsaccade behaviors and adopt a microsaccade bias towards the seeing field might have better visual perception. New microsaccade patterns allow patients to make better use of the visual capacities they still have. Our findings justify microsaccade testing as part of the routine visual function assessments in hemianopia. Future methods are needed to monitor or modulate microsaccade to open new avenues for vision restoration and rehabilitation. Microsaccades may be tiny, but not too tiny to care.

5. General discussion

The present series of studies investigated microsaccades' physiological responses and their impacts on brain oscillations and brain functional connectivity network dynamics. I propose that they play a significant role in vision not only through retinal refreshment, but also "cortical refreshment". Assessment of microsaccade features across the life span revealed that microsaccades and their physiological responses were stable during aging, which suggests their potential as a biomarker in diagnosing and monitoring diseases with relevant symptoms. In hemianopia after stroke, the present results evidenced the alterations of microsaccades and their relationships with visual functions and disease features, which legitimize the routine assessment of microsaccades in hemianopia and more studies on their role in vision rehabilitation and restoration.

5.1.   Microsaccades cortical refreshment

Microsaccades have been proposed to counteract photoreceptor adaptation and refresh retinal images (Engbert & Mergenthaler, 2006). Through retinal refreshment, they are believed to play a significant role in high-acuity and clear vision. Now we show that besides retinal refreshment, microsaccades modulate brain status as well, which I termed "cortical refreshment". Firstly, microsaccades reset alpha band phase globally within the MLR window (100-200 ms after microsaccade onset). The alpha wave phase can determine whether a stimuli reaches sensory awareness or not (Busch et al., 2009; Busch & VanRullen, 2010; Mathewson et al., 2009). This finding supports the view that eye movements' corollary activity is closely related to anticipatory preparation of visual centers for visual processing (Melloni et al., 2009).

Secondly, the global efficiency of alpha band brain functional network was enhanced from 200 ms before microsaccade onset to around 160 ms after it. The alpha band brain functional network was proposed to play an attentional role in vision. It

supports active processing of task-relevant information and inhibits task-irrelevant neuronal activity (Palva & Palva, 2011). By optimizing attention allocation, alpha band brain functional network is critical in determining what information gets the most processing resources, which in the next step influences higher cognitive functions utilizing the products of this visual processing. By enhancing remote communication efficiency in the brain, microsaccades facilitate the coordination of this attention system.

To sum up, through synchronizing alpha band phase globally and enhancing communication efficiency of the alpha band brain functional network, microsaccades can prepare (sensitize) the brain to optimize subsequent visual processing. Such cortical refreshment is another mechanism underlying microsaccdaes' critical role in vision.

5.2.   Microsaccades' potential as a biomarker

Microsaccades are highly clinically relevant. Alterations of microsaccades are closely related to subjective visual impairments, such as blurred (foggy) vision and diplopia (Ciuffreda & Tannen, 1995; Foroozan & Brodsky, 2004). These subjective visual impairments are commonly reported in diseases such as Glaucoma and hemianopia (G. A. de Haan et al., 2015; Poggel et al., 2007; Rowe et al., 2013). Evaluation of microsaccade function can help understanding, diagnosing and monitoring these diseases. On the other hand, the control circuits of microsaccades include multiple cortical regions such as the frontal eye field, the supplementary eye field, the prefrontal eye field, the parietal eye field, all of which are highly connected with other visual system structures (Figure 1.11) (Lynch, 2009). A microsaccade is a product of a successfully coordinated network. Medical conditions disturbing brain functional network could be probed by microsaccade assessment.

A series of studies investigated the microsaccade alterations in several ophthalmological and neurological diseases. In amblyopia patients, amblyopic eyes conducted fewer but larger and faster microsaccades than the control eyes (Shi et al., 2012). Because of brainstem and/or cerebellum impairment, PSP patients display more

frequent, slowed and enlarged microsaccade amplitude and a loss of the vertical component (Otero-Millan, Schneider, et al., 2013; Otero-Millan et al., 2011b). In patients with PD, increased fluctuations in SC activity raise the microsaccade rates (Otero-Millan, Schneider, et al., 2013). In AD and MCI, altered microsaccade direction was observed, which might be related to attentional deficiencies (Kapoula et al., 2014). These diseases often occur in different age groups, particularly in the elderly population. Within one study, the age range of the patients can be wide as well. Thus, it is crucial to know if microsaccades are age-dependent to appreciate the impact of these diseases on microsaccades. We found that microsaccade and microsaccade-related potentials were stable across the life span. This stability is an excellent condition so that microsaccades can serve as reference points when studying age-associated neurodegenerative or neuro-ophthalmological diseases with oculomotor symptoms.

5.3. Microsaccades are important for hemianopia: diagnosis and rehabilitation

We report the first comprehensive assessment of microsaccade features in patients with homonymous hemianopia and their relation with lesion age, visual field defect topography and visual performances. We found microsaccades to be enlarged in amplitude, prolonged in duration and impaired in their binocular conjugacy. These alterations were more severe in patients with older lesions, suggesting that these alterations are the consequence of the enduring experience of the vision loss, rather than a direct consequence of the brain damage and the associated acute visual field loss. Yet, microsaccade velocity was not significantly different from that of control subjects, indicating that motor aspects of eye movement generation were preserved after our patients had their posterior artery stroke damage (Shakespeare et al., 2015). Hemianopic patients did not show a microsaccade direction bias towards the deficit area as we hypothesized. Interestingly, half of our patients showed a microsaccade direction bias towards the seeing field and exhibited faster stimulus detection in ARVs. In addition, patients with a greater number of binocular microsaccades and slower

microsaccade velocity performed better in visual acuity tests.

Evaluating microsaccades in hemianopia is necessary for diagnosis and monitoring the condition. Hemianopic patients' binocular microsaccade percentage and microsaccade velocity correlate with their visual acuity. Microsaccade parameters can add critical information to a comprehensive description of the visual impairments after stroke. In hemianopia, visual field defects deprive the SC of visual input, which may cause insufficient inhibition by the SC, resulting in microsaccade enlargement and prolongation. Binocular conjugacy of microsaccades was also impaired, which suggests malfunctioning calibration of this eye movement control system due to a disturbed brain functional connectivity network after stroke and the deprivation of visual input that play a significant role in optimizing the system. These alterations were more severe in patients with older lesions, which supports the idea that routine microsaccade tests can help monitor the disease progress (even when the lesion in the brain is stable) to plan better rehabilitation.

From microsaccade alterations, we can learn to design new rehabilitation methods. Half of the hemianopia group showed a microsaccade direction bias towards the intact area, while the other half showed no direction bias. The biased group detected visual stimuli faster in ARVs compared to the non-biased group. We hypothesize that a microsaccade direction bias in about half of the hemianopic patients is a sign of a greater allocation of attention towards their seeing field (including ARVs). Such an adaptive attention allocation in the ARVs may be the cause why such patients had faster reaction times in ARVs. This is a strategy different from that of macrosaccades. This may be due to their different functions in normal vision. Whereas in hemianopia macrosaccades (1-30 degrees of visual angle) are used to move objects located in the deficit area into to the intact visual field, microsaccades are very small (up to 1 degree) and their function is rather to refresh vision, prevent fading, and serve as a sampling tool in a relative small and more local region of the visual field. We propose that whereas macrosaccades help to capture visual scenes on the deficit side in hemianopia, microsaccades are adaptive for visual perception itself and thus improve acuity and

visual performance in the intact and in the partially damaged visual field. This gives us an insight that while designing eye movement training for hemianopic patients, we should utilize different strategies in different tasks emphasizing general viewing, object search, or small-scale scanning.

But further studies are needed to clarify the visual functions and performance differences between patients with different microsaccade patterns to be able to determine which elements are maladaptive and which are adaptive for vision.

5.4. Methodological considerations and limitations

Here, I also mention several methodological limitations of this work for helping the design of future studies.

In study II, microsaccades' impacts on brain oscillations and functional network were revealed and the mechanism of cortical refreshment was proposed. However, the present study did not provide evidence of the relationship between these physiological responses and behavioral visual performance. Future studies showing the correlation between microsaccade-related brain status and behavioral performance fluctuation would add critical evidence to this hypothesis.

Considering EEG analysis methods, source based data after source reconstruction was used for functional connectivity network analysis, and the imaginary part of coherence was used to calculate the functional coupling between different sources. These two techniques can help reduce the interference of volume conductance to some extent. Future studies combining functional Magnetic Resonance Imaging (fMRI) and high-density EEG will be able to provide more reliable functional connectivity information with both high temporal and spatial resolutions.

In study III, only eye tracking data was recorded from hemianopic patients due to the technical limitation at that time. Future studies utilizing combined eye tracking and EEG recording can reveal how microsaccade-related potentials, spectral power and

phase dynamic, and brain functional connectivity network features are altered in hemianopia after stroke, and how these alterations influence patients' visual performance.

6. Microsaccades refresh the brain status: a new mechanism underlying clear vision

Microsaccades' function in facilitating clear vision has been accepted more widely in recent years (Martinez-Conde et al., 2013; Rolfs, 2009). Microsaccades were proposed to reduce perceptual fading, and to be able to better maintain fixation accuracy. However, these functions were not exclusive for microsaccades, but can be achieved by other eye movements as well (e.g. drift). Yet, microsaccades' role in visual perception is not sufficiently understood. But the findings of my present study suggest an interesting, new mechanism of microsaccade function. Namely, I propose that cortical refreshment is a hitherto unknown and new mechanism of how microsaccades improve vision.

Besides reducing perceptual fading and oculomotor control, microsaccades induce a kind of "reset" of the brain´s physiological state in temporal, spectral and functional connectivity network domains. Specically, these changes are as follows:

(i) In the temporal domain, microsaccades evoked MLR, which is similar to VEP, represents the cortical activation caused by the transient retinal image slip. This suggests that microsaccades can introduce a stimulus/signal to the visual system even when there is no new stimulus in the environment.

(ii) In the spectral domain, microsaccades induced occipital alpha band perturbation and global alpha band phase synchronization. The alpha wave phase can determine whether a stimulus reaches sensory awareness or not (Busch et al., 2009; Busch & VanRullen, 2010; Mathewson et al., 2009). By interacting with alpha waves in the brain, microsaccades can modulate the brain to achieve an optimized status for visual processing.

(iii) In the functional connectivity network domain, microsaccades enhanced both local and global efficiency of alpha band brain functional network. This suggests that

microsaccade can enhance the regional and remote communication in the brain from time to time at its own pace. The alpha band brain functional network was proposed to play an important role of modulating or mediating visual attention. Given that attention supports active processing of task-relevant information and inhibits task-irrelevant neuronal activity (Palva & Palva, 2011), I propose that, microsaccades can modulate the regional and remote communication in the brain to update attention allocation at its own pace.

To sum up, microsaccades' consequences include visual cortex activation, global alpha band phase synchronization and alpha band functional connectivity network efficiency enhancement. Microsaccades refresh the brain status at its own pace to facilitate visual processing, which I wish to term "cortical refreshment". I believe my new findings are critical in understanding microsaccades' function in normal and abnormal vision. This might benefit visual system research and it may offer new options for visual enhancement and vision restoration in low vision.

7. References

Abel, L. A., & Douglas, J. (2007). Effects of age on latency and error generation in internally mediated saccades. *Neurobiology of Aging, 28*(4), 627-637.

Abel, L. A., Troost, B. T., & Dell'Osso, L. F. (1983). The effects of age on normal saccadic characteristics and their variability. *Vision Research, 23*(1), 33-37.

Bahnemann, M., Hamel, J., De Beukelaer, S., Ohl, S., Kehrer, S., Audebert, H., Kraft, A., & Brandt, S. A. (2014). Compensatory eye and head movements of patients with homonymous hemianopia in the naturalistic setting of a driving simulation. *Journal of Neurology, 262*, 316-325. doi:10.1007/s00415-014-7554-x

Bassett, D. S., & Bullmore, E. (2006). Small-world brain networks. *The Neuroscientist, 12*(6), 512-523.

Benedetto, S., Pedrotti, M., & Bridgeman, B. (2011). Microsaccades and exploratory saccades in a naturalistic environment. *Journal of Eye Movement Research, 4*(2), 1-10.

Bola, M., Gall, C., Moewes, C., Fedorov, A., Hinrichs, H., & Sabel, B. A. (2014). Brain functional connectivity network breakdown and restoration in blindness. *Neurology, 83*(6), 542-551.

Bola, M., Gall, C., & Sabel, B. A. (2013a). The second face of blindness: processing speed deficits in the intact visual field after pre-and post-chiasmatic lesions. *PLoS One, 8*(5), e63700.

Bola, M., Gall, C., & Sabel, B. A. (2013b). Sightblind": perceptual deficits in the "intact" visual field. *Frontiers in Neurology, 4*, 80.

Bola, M., Gall, C., & Sabel, B. A. (2015). Disturbed temporal dynamics of brain synchronization in vision loss. *Cortex, 67*, 134-146.

Bosman, C. A., Womelsdorf, T., Desimone, R., & Fries, P. (2009). A microsaccadic rhythm modulates gamma-band synchronization and behavior. *Journal of Neuroscience, 29*(30), 9471-9480.

Bridgeman, B., & Palca, J. (1980). The role of microsaccades in high acuity observational tasks. *Vision Research, 20*(9), 813-817.

Bullmore, E., & Sporns, O. (2009). Complex brain networks: graph theoretical analysis of structural and functional systems. *Nature Reviews Neuroscience, 10*(3), 186.

Busch, N. A., Dubois, J., & VanRullen, R. (2009). The phase of ongoing EEG oscillations predicts visual perception. *Journal of Neuroscience, 29*(24), 7869-7876.

Busch, N. A., & VanRullen, R. (2010). Spontaneous EEG oscillations reveal periodic sampling of visual attention. *Proceedings of the National Academy of Sciences, 107*(37), 16048-16053.

Butler, K. M., Zacks, R. T., & Henderson, J. M. (1999). Suppression of reflexive saccades in younger and older adults: Age comparisons on an antisaccade task. *Memory & Cognition, 27*(4), 584-591.

Campbell, K. L., Al-Aidroos, N., Pratt, J., & Hasher, L. (2009). Repelling the young and attracting the old: examining age-related differences in saccade trajectory deviations. *Psychology and Aging, 24*(1), 163-168.

Carter, A. R., Patel, K. R., Astafiev, S. V., Snyder, A. Z., Rengachary, J., Strube, M. J., Pope, A., Shimony, J. S., Lang, C. E., & Shulman, G. L. (2012). Upstream dysfunction of somatomotor functional connectivity after corticospinal damage in stroke. *Neurorehabilitation and Neural Repair, 26*(1), 7-19.

Carter, J. E., Obler, L., Woodward, S., & Albert, M. L. (1983). The effect of increasing age on the latency for saccadic eye movements. *Journal of Gerontology, 38*(3), 318-320.

Catani, M., Dell'Acqua, F., Bizzi, A., Forkel, S. J., Williams, S. C., Simmons, A., Murphy, D. G., & De Schotten, M. T. (2012). Beyond cortical localization in clinico-anatomical correlation. *Cortex, 48*(10), 1262-1287.

Chen, P. L., & Machado, L. (2016). Age-related deficits in voluntary control over saccadic eye movements: consideration of electrical brain stimulation as a therapeutic strategy. *Neurobiology of Aging, 41*, 53-63.

Ciuffreda, K. J., & Tannen, B. (1995). *Eye movement basics for the clinician*: Mosby Incorporated.

Connolly, J., & Gruzelier, J. H. (1982). Amplitude and latency changes in the visual evoked potential to different stimulus intensities. *Psychophysiology, 19*(6), 599-608.

Costela, F., Otero-Millan, J., McCamy, M., Macknik, S., Troncoso, X., & Martinez-Conde, S. (2013). Microsaccades correct fixation errors due to blinks. *Journal of Vision, 13*(9), 1335-1335.

de Haan, E. H., & Cowey, A. (2011). On the usefulness of 'what' and 'where' pathways in vision. *Trends in Cognitive Sciences, 15*(10), 460-466.

de Haan, G. A., Heutink, J., Melis-Dankers, B. J. M., Brouwer, W. H., & Tucha, O. (2015). Difficulties in Daily Life Reported by Patients With Homonymous Visual Field Defects. *Journal of Neuro-Ophthalmology, 35*, 259-264. doi:10.1097/WNO.0000000000000244

Delorme, A., & Makeig, S. (2004). EEGLAB: an open source toolbox for analysis of single-trial EEG dynamics including independent component analysis. *Journal of Neuroscience Methods, 134*(1), 9-21.

Desikan, R. S., Ségonne, F., Fischl, B., Quinn, B. T., Dickerson, B. C., Blacker, D., Buckner, R. L., Dale, A. M., Maguire, R. P., & Hyman, B. T. (2006). An automated labeling system for subdividing the human cerebral cortex on MRI scans into gyral based regions of interest. *Neuroimage, 31*(3), 968-980.

Dimigen, O., Sommer, W., Hohlfeld, A., Jacobs, A. M., & Kliegl, R. (2011). Coregistration of eye movements and EEG in natural reading: analyses and review. *Journal of Experimental Psychology: General, 140*(4), 552-572.

Dimigen, O., Valsecchi, M., Sommer, W., & Kliegl, R. (2009). Human microsaccade-related visual brain responses. *Journal of Neuroscience, 29*(39), 12321-12331.

Donner, K., & Hemilä, S. (2007). Modelling the effect of microsaccades on retinal

responses to stationary contrast patterns. *Vision Research, 47*(9), 1166-1177.

Engbert, R. (2006). Microsaccades: A microcosm for research on oculomotor control, attention, and visual perception. *Progress in Brain Research, 154*, 177-192.

Engbert, R., & Kliegl, R. (2003). Microsaccades uncover the orientation of covert attention. *Vision Research, 43*(9), 1035-1045.

Engbert, R., & Kliegl, R. (2004). Microsaccades keep the eyes' balance during fixation. *Psychological Science, 15*(6), 431-431.

Engbert, R., & Mergenthaler, K. (2006). Microsaccades are triggered by low retinal image slip. *Proceedings of the National Academy of Sciences, 103*(18), 7192-7197.

Fallani, F. D. V., Astolfi, L., Cincotti, F., Mattia, D., Marciani, M. G., Salinari, S., Kurths, J., Gao, S., Cichocki, A., & Colosimo, A. (2007). Cortical functional connectivity networks in normal and spinal cord injured patients: evaluation by graph analysis. *Human Brain Mapping, 28*(12), 1334-1346.

Foroozan, R., & Brodsky, M. C. (2004). Microsaccadic opsoclonus: an idiopathic cause of oscillopsia and episodic blurred vision. *American Journal of Ophthalmology, 138*(6), 1053-1054.

Friston, K., Frith, C., & Frackowiak, R. (1993). Time‐dependent changes in effective connectivity measured with PET. *Human Brain Mapping, 1*(1), 69-79.

Gall, C., Franke, G. H., & Sabel, B. A. (2010). Vision-related quality of life in first stroke patients with homonymous visual field defects. *Health and Quality of Life Outcomes, 8*(1), 1.

Gall, C., Lucklum, J., Sabel, B. A., & Franke, G. H. (2009). Vision-and health-related quality of life in patients with visual field loss after postchiasmatic lesions. *Investigative Ophthalmology & Visual Science, 50*(6), 2765-2776.

Gall, C., Mueller, I., Kaufmann, C., Franke, G., & Sabel, B. A. (2008). [Visual field defects after cerebral lesions from the patient's perspective: health-and vision-related quality of life assessed by SF-36 and NEI-VFQ]. *Der Nervenarzt, 79*(2), 185-194.

Gao, Y., & Sabel, B. (2017). Microsaccade dysfunction and adaptation in hemianopia after stroke. *Restorative Neurology and Neuroscience, 35*(4), 365-376. doi:10.3233/RNN-170749

Gottlob, L. R., Fillmore, M. T., & Abroms, B. D. (2007). Age-group differences in saccadic interference. *The Journals of Gerontology Series B: Psychological Sciences and Social Sciences, 62*(2), P85-P89.

Gramfort, A., Papadopoulo, T., Olivi, E., & Clerc, M. (2010). OpenMEEG: opensource software for quasistatic bioelectromagnetics. *Biomedical Engineering Online, 9*(1), 45.

Grefkes, C., Nowak, D. A., Eickhoff, S. B., Dafotakis, M., Küst, J., Karbe, H., & Fink, G. R. (2008). Cortical connectivity after subcortical stroke assessed with functional magnetic resonance imaging. *Annals of Neurology, 63*(2), 236-

246.

Hafed, Z. M., & Clark, J. J. (2002). Microsaccades as an overt measure of covert attention shifts. *Vision Research, 42*(22), 2533-2545.

Hafed, Z. M., Goffart, L., & Krauzlis, R. J. (2009). A neural mechanism for microsaccade generation in the primate superior colliculus. *Science, 323*(5916), 940-943.

Hämäläinen, M. S., & Ilmoniemi, R. J. (1994). Interpreting magnetic fields of the brain: minimum norm estimates. *Medical and Biological Engineering and Computing, 32*(1), 35-42.

Hamel, J., De Beukelear, S., Kraft, A., Ohl, S., Audebert, H. J., & Brandt, S. A. (2013). Age-related changes in visual exploratory behavior in a natural scene setting. *Frontiers in Psychology, 4*, 339.

Herrmann, C. S., Rach, S., Vosskuhl, J., & Strüber, D. (2014). Time–frequency analysis of event-related potentials: a brief tutorial. *Brain Topography, 27*(4), 438-450.

Hess, R., & Pointer, J. (1989). Spatial and temporal contrast sensitivity in hemianopia: a comparative study of the sighted and blind hemifields. *Brain, 112*(4), 871-894.

Huddleston, W. E., Ernest, B. E., & Keenan, K. G. (2014). Selective age effects on visual attention and motor attention during a cued saccade task. *Journal of Ophthalmology, 2014*, 860493.

Kapoula, Z., Yang, Q., Otero-Millan, J., Xiao, S., Macknik, S. L., Lang, A., Verny, M., & Martinez-Conde, S. (2014). Distinctive features of microsaccades in Alzheimer's disease and in mild cognitive impairment. *Age, 36*(2), 535-543.

Kasten, E., Strasburger, H., & Sabel, B. A. (1997). Programs for diagnosis and therapy of visual field deficits in vision rehabilitation. *Spatial Vision, 10*, 499-503.

Kerber, K. A., Ishiyama, G. P., & Baloh, R. W. (2006). A longitudinal study of oculomotor function in normal older people. *Neurobiology of Aging, 27*(9), 1346-1353.

Klein, C., Fischer, B., Hartnegg, K., Heiss, W., & Roth, M. (2000). Optomotor and neuropsychological performance in old age. *Experimental Brain Research, 135*(2), 141-154.

Klein, C., Foerster, F., Hartnegg, K., & Fischer, B. (2005). Lifespan development of pro-and anti-saccades: multiple regression models for point estimates. *Developmental Brain Research, 160*(2), 113-123.

Ko, H.-k., Poletti, M., & Rucci, M. (2010). Microsaccades precisely relocate gaze in a high visual acuity task. *Nature Neuroscience, 13*(12), 1549-1553.

Kommerell, G., Lieb, B., & Münßinger, U. (1999). Rehabilitation bei homonymer Hemianopsie. *Z prakt Augenheilkd, 20*, 344-352.

Kuba, M., Kremláček, J., Langrová, J., Kubová, Z., Szanyi, J., & Vít, F. (2012). Aging effect in pattern, motion and cognitive visual evoked potentials. *Vision Research, 62*, 9-16.

Kybic, J., Clerc, M., Abboud, T., Faugeras, O., Keriven, R., & Papadopoulo, T. (2005).

A common formalism for the integral formulations of the forward EEG problem. *IEEE Transactions on Medical Imaging, 24*(1), 12-28.

Lakatos, P., O'Connell, M. N., Barczak, A., Mills, A., Javitt, D. C., & Schroeder, C. E. (2009). The leading sense: supramodal control of neurophysiological context by attention. *Neuron, 64*(3), 419-430.

Lin, F. H., Belliveau, J. W., Dale, A. M., & Hämäläinen, M. S. (2006). Distributed current estimates using cortical orientation constraints. *Human Brain Mapping, 27*(1), 1-13.

Litvinova, A., Ratmanova, P., Evina, E., Bogdanov, R., Kunitsyna, A., & Napalkov, D. (2011). Age-related changes in saccadic eye movements in healthy subjects and patients with Parkinson's disease. *Human Physiology, 37*(2), 161.

Liversedge, S., Gilchrist, I., & Everling, S. (2011). *The Oxford Handbook of Eye Movements*: Oxford University Press.

Lowet, E., Roberts, M., Bosman, C., Fries, P., & De Weerd, P. (2016). Areas V1 and V2 show microsaccade‐related 3–4‐Hz covariation in gamma power and frequency. *European Journal of Neuroscience, 43*(10), 1286-1296.

Lynch, J. (2009). Oculomotor control: anatomical pathways. *Encyclopedia of Neuroscience, 7*, 17-23.

Makeig, S. (1993). Auditory event-related dynamics of the EEG spectrum and effects of exposure to tones. *Electroencephalography and Clinical Neurophysiology, 86*(4), 283-293.

Makeig, S., Debener, S., Onton, J., & Delorme, A. (2004). Mining event-related brain dynamics. *Trends in Cognitive Sciences, 8*(5), 204-210.

Martinez-Conde, S. (2006). Fixational eye movements in normal and pathological vision. *Progress in Brain Research, 154*, 151-176.

Martinez-Conde, S., & Macknik, S. L. (2008). Fixational eye movements across vertebrates: comparative dynamics, physiology, and perception. *Journal of Vision, 8*(14), 28-28.

Martinez-Conde, S., Macknik, S. L., & Hubel, D. H. (2004). The role of fixational eye movements in visual perception. *Nature Reviews Neuroscience, 5*(3), 229-240.

Martinez-Conde, S., Macknik, S. L., Troncoso, X. G., & Hubel, D. H. (2009). Microsaccades: a neurophysiological analysis. *Trends in Neurosciences, 32*(9), 463-475.

Martinez-Conde, S., Otero-Millan, J., & Macknik, S. L. (2013). The impact of microsaccades on vision: towards a unified theory of saccadic function. *Nature Reviews Neuroscience, 14*(2), 83-96.

Mathewson, K. E., Gratton, G., Fabiani, M., Beck, D. M., & Ro, T. (2009). To see or not to see: prestimulus α phase predicts visual awareness. *Journal of Neuroscience, 29*(9), 2725-2732.

Matiño-Soler, E., Esteller-More, E., Martin-Sanchez, J.-C., Martinez-Sanchez, J.-M., & Perez-Fernandez, N. (2015). Normative data on angular vestibulo-ocular responses in the yaw axis measured using the video head impulse test. *Otology & Neurotology, 36*(3), 466-471.

McCamy, M. B., Otero-Millan, J., Macknik, S. L., Yang, Y., Troncoso, X. G., Baer, S. M., Crook, S. M., & Martinez-Conde, S. (2012). Microsaccadic efficacy and contribution to foveal and peripheral vision. *The Journal of Neuroscience, 32*(27), 9194-9204.

Meienberg, O., Zangemeister, W. H., Rosenberg, M., Hoyt, W. F., & Stark, L. (1981). Saccadic eye movement strategies in patients with homonymous hemianopia. *Annals of Neurology, 9*(6), 537-544.

Melloni, L., Schwiedrzik, C. M., Rodriguez, E., & Singer, W. (2009). (Micro) Saccades, corollary activity and cortical oscillations. *Trends in Cognitive Sciences, 13*(6), 239-245.

Meyberg, S., Werkle-Bergner, M., Sommer, W., & Dimigen, O. (2015). Microsaccade-related brain potentials signal the focus of visuospatial attention. *NeuroImage, 104*, 79-88.

Moschner, C., & Baloh, R. W. (1994). Age-related changes in visual tracking. *Journal of Gerontology, 49*(5), M235-M238.

Munoz, D., Broughton, J., Goldring, J., & Armstrong, I. (1998). Age-related performance of human subjects on saccadic eye movement tasks. *Experimental Brain Research, 121*(4), 391-400.

Nash-Kille, A., & Sharma, A. (2014). Inter-trial coherence as a marker of cortical phase synchrony in children with sensorineural hearing loss and auditory neuropathy spectrum disorder fitted with hearing aids and cochlear implants. *Clinical Neurophysiology, 125*(7), 1459-1470.

Nelles, G., Esser, J., Eckstein, A., Tiede, A., Gerhard, H., & Diener, H. C. (2001). Compensatory visual field training for patients with hemianopia after stroke. *Neuroscience Letters, 306*(3), 189-192.

Nottage, J. F., & Horder, J. (2015). State-of-the-art analysis of high-frequency (gamma range) electroencephalography in humans. *Neuropsychobiology, 72*, 219-228.

Olincy, A., Ross, R., Youngd, D., & Freedman, R. (1997). Age diminishes performance on an antisaccade eye movement task. *Neurobiology of Aging, 18*(5), 483-489.

Otero-Millan, J., Macknik, S. L., Langston, R. E., & Martinez-Conde, S. (2013). An oculomotor continuum from exploration to fixation. *Proceedings of the National Academy of Sciences, 110*(15), 6175-6180.

Otero-Millan, J., Schneider, R., Leigh, R. J., Macknik, S. L., & Martinez-Conde, S. (2013). Saccades during attempted fixation in parkinsonian disorders and recessive ataxia: From microsaccades to square-wave jerks. *PLoS One, 8*(3), e58535.

Otero-Millan, J., Serra, A., Leigh, R. J., Troncoso, X. G., Macknik, S. L., & Martinez-Conde, S. (2011a). Distinctive features of saccadic intrusions and microsaccades in progressive supranuclear palsy. *The Journal of Neuroscience, 31*(12), 4379-4387.

Otero-Millan, J., Serra, A., Leigh, R. J., Troncoso, X. G., Macknik, S. L., & Martinez-Conde, S. (2011b). Distinctive features of saccadic intrusions and

microsaccades in progressive supranuclear palsy. *Journal of Neuroscience, 31*(12), 4379-4387.

Otero-Millan, J., Troncoso, X. G., Macknik, S. L., Serrano-Pedraza, I., & Martinez-Conde, S. (2008). Saccades and microsaccades during visual fixation, exploration, and search: foundations for a common saccadic generator. *Journal of Vision, 8*(14), 21-21.

Otero‐Millan, J., Macknik, S. L., Serra, A., Leigh, R. J., & Martinez‐Conde, S. (2011). Triggering mechanisms in microsaccade and saccade generation: a novel proposal. *Annals of the New York Academy of Sciences, 1233*(1), 107-116.

Palva, S., & Palva, J. M. (2011). Functional roles of alpha-band phase synchronization in local and large-scale cortical networks. *Frontiers in Psychology, 2*, 204.

Pambakian, A. L. M., Wooding, D., Patel, N., Morland, A., Kennard, C., & Mannan, S. (2000). Scanning the visual world: a study of patients with homonymous hemianopia. *Journal of Neurology, Neurosurgery & Psychiatry, 69*(6), 751-759.

Papageorgiou, E., Hardiess, G., Schaeffel, F., Wiethoelter, H., Karnath, H.-O., Mallot, H., Schoenfisch, B., & Schiefer, U. (2007). Assessment of vision-related quality of life in patients with homonymous visual field defects. *Graefe's Archive for Clinical and Experimental Ophthalmology, 245*(12), 1749-1758.

Paramei, G. V., & Sabel, B. A. (2008). Contour-integration deficits on the intact side of the visual field in hemianopia patients. *Behavioural Brain Research, 188*(1), 109-124.

Pastukhov, A., Vonau, V., Stonkute, S., & Braun, J. (2013). Spatial and temporal attention revealed by microsaccades. *Vision Research, 85*, 45-57.

Peltsch, A., Hemraj, A., Garcia, A., & Munoz, D. (2011). Age-related trends in saccade characteristics among the elderly. *Neurobiology of Aging, 32*(4), 669-679.

Pitt, M., & Rawles, J. (1988). The effect of age on saccadic latency and velocity. *Neuro-Ophthalmology, 8*(3), 123-129.

Poggel, D. A., Kasten, E., Müller-Oehring, E. M., Bunzenthal, U., & Sabel, B. A. (2006). Improving residual vision by attentional cueing in patients with brain lesions. *Brain Research, 1097*(1), 142-148.

Poggel, D. A., Kasten, E., & Sabel, B. A. (2004). Attentional cueing improves vision restoration therapy in patients with visual field defects. *Neurology, 63*(11), 2069-2076.

Poggel, D. A., Müller-Oehring, E., Gothe, J., Kenkel, S., Kasten, E., & Sabel, B. A. (2007). Visual hallucinations during spontaneous and training-induced visual field recovery. *Neuropsychologia, 45*(11), 2598-2607.

Poggel, D. A., Treutwein, B., & Strasburger, H. (2011). Time will tell: deficits of temporal information processing in patients with visual field loss. *Brain Research, 1368*, 196-207.

Poletti, M., Listorti, C., & Rucci, M. (2013). Microscopic eye movements compensate for nonhomogeneous vision within the fovea. *Current Biology, 23*(17), 1691-1695.

Populin, L. C. (2005). Anesthetics change the excitation/inhibition balance that governs sensory processing in the cat superior colliculus. *The Journal of Neuroscience, 25*(25), 5903-5914.

Port, N. L., Trimberger, J., Hitzeman, S., Redick, B., & Beckerman, S. (2016). Micro and regular saccades across the lifespan during a visual search of "Where's Waldo" puzzles. *Vision Research, 118*, 144-157.

Pratt, J., Dodd, M., & Welsh, T. (2006). Growing older does not always mean moving slower: examining aging and the saccadic motor system. *Journal of Motor Behavior, 38*(5), 373-382.

Raemaekers, M., Vink, M., van den Heuvel, M. P., Kahn, R. S., & Ramsey, N. F. (2006). Effects of aging on BOLD fMRI during prosaccades and antisaccades. *Journal of Cognitive Neuroscience, 18*(4), 594-603.

Raz, N., Dotan, S., Benoliel, T., Chokron, S., Ben-Hur, T., & Levin, N. (2011). Sustained motion perception deficit following optic neuritis Behavioral and cortical evidence. *Neurology, 76*(24), 2103-2111.

Raz, N., Dotan, S., Chokron, S., Ben‐Hur, T., & Levin, N. (2012). Demyelination affects temporal aspects of perception: an optic neuritis study. *Annals of Neurology, 71*(4), 531-538.

Reinhard, J. I., Damm, I., Ivanov, I. V., & Trauzettel-Klosinski, S. (2014). Eye Movements During Saccadic and Fixation Tasks in Patients With Homonymous Hemianopia. *Journal of Neuro-Ophthalmology, 34*, 354-361. doi:10.1097/WNO.0000000000000146

Rizzo, M., & Robin, D. A. (1996). Bilateral effects of unilateral visual cortex lesions in human. *Brain, 119*(3), 951-963.

Rolfs, M. (2009). Microsaccades: small steps on a long way. *Vision Research, 49*(20), 2415-2441.

Rowe, F., Brand, D., Jackson, C. A., Price, A., Walker, L., Harrison, S., Eccleston, C., Scott, C., Akerman, N., & Dodridge, C. (2009). Visual impairment following stroke: do stroke patients require vision assessment? *Age and Ageing, 38*(2), 188-193.

Rowe, F., Wright, D., Brand, D., Jackson, C., Harrison, S., Maan, T., Scott, C., Vogwell, L., Peel, S., & Akerman, N. (2013). A prospective profile of visual field loss following stroke: prevalence, type, rehabilitation, and outcome. *BioMed Research International, 2013*, 1-12.

Rubinov, M., & Sporns, O. (2010). Complex network measures of brain connectivity: uses and interpretations. *Neuroimage, 52*(3), 1059-1069.

Sabel, B. A. (2016). Restoring Low Vision: How to strengthen your potentials in low vision and blindness. .

Sabel, B. A., Henrich-Noack, P., Fedorov, A., & Gall, C. (2011). Vision restoration after brain and retina damage: the "residual vision activation theory". *Progress in Brain Research, 192*(1), 199-262.

Sabel, B. A., Kenkel, S., & Kasten, E. (2004). Vision restoration therapy (VRT) efficacy as assessed by comparative perimetric analysis and subjective questionnaires. *Restorative Neurology and Neuroscience, 22*, 399-420.

Sand, K., Midelfart, A., Thomassen, L., Melms, A., Wilhelm, H., & Hoff, J. (2013). Visual impairment in stroke patients–a review. *Acta Neurologica Scandinavica, 127*(s196), 52-56.

Schadow, J., Dettler, N., Paramei, G. V., Lenz, D., Fründ, I., Sabel, B. A., & Herrmann, C. S. (2009). Impairments of Gestalt perception in the intact hemifield of hemianopic patients are reflected in gamma-band EEG activity. *Neuropsychologia, 47*(2), 556-568.

Schik, G., Mohr, S., & Hofferberth, B. (2000). Effect of aging on saccadic eye movements to visual and auditory targets. *International Tinnitus Journal, 6*(2), 154-159.

Schneider, R. M., Thurtell, M. J., Eisele, S., Lincoff, N., Bala, E., & Leigh, R. J. (2013). Neurological basis for eye movements of the blind. *PloS One, 8*(2), e56556.

Schwartzman, D. J., & Kranczioch, C. (2011). In the blink of an eye: the contribution of microsaccadic activity to the induced gamma band response. *International Journal of Psychophysiology, 79*(1), 73-82.

Shakespeare, T. J., Kaski, D., Yong, K. X., Paterson, R. W., Slattery, C. F., Ryan, N. S., Schott, J. M., & Crutch, S. J. (2015). Abnormalities of fixation, saccade and pursuit in posterior cortical atrophy. *Brain, 138*(7), 1976-1991.

Sharpe, J. A., & Zackon, D. H. (1987). Senescent saccades: effects of aging on their accuracy, latency and velocity. *Acta Oto-laryngologica, 104*(5-6), 422-428.

Shi, X.-f. F., Xu, L.-m., Li, Y., Wang, T., Zhao, K.-x., & Sabel, B. A. (2012). Fixational saccadic eye movements are altered in anisometropic amblyopia. *Restorative Neurology and Neuroscience, 30*(6), 445-462.

Singer, W. (1996). Neuronal synchronization: A solution to the binding problem. *The Mind–Brain Continuum: Sensory Processes*, 101-130.

Spooner, J. W., Sakala, S. M., & Baloh, R. W. (1980). Effect of aging on eye tracking. *Archives of Neurology, 37*(9), 575-576.

Sweeney, J. A., Rosano, C., Berman, R. A., & Luna, B. (2001). Inhibitory control of attention declines more than working memory during normal aging. *Neurobiology of Aging, 22*(1), 39-47.

Tadel, F., Baillet, S., Mosher, J. C., Pantazis, D., & Leahy, R. M. (2011). Brainstorm: a user-friendly application for MEG/EEG analysis. *Computational Intelligence and Neuroscience, 2011*, 8.

Tedeschi, G., Di Costanzo, A., Allocca, S., Quattrone, A., Casucci, G., Russo, L., & Bonavita, V. (1988). Age-dependent changes in visually guided saccadic eye movements. *Functional neurology, 4*(4), 363-367.

Triplett, J. W., Owens, M. T., Yamada, J., Lemke, G., Cang, J., Stryker, M. P., & Feldheim, D. A. (2009). Retinal input instructs alignment of visual topographic maps. *Cell, 139*(1), 175-185.

Van Essen, D. C., Anderson, C. H., & Felleman, D. J. (1992). Information processing in the primate visual system: an integrated systems perspective. *Science, 255*(5043), 419-423.

Warabi, T., Kase, M., & Kato, T. (1984). Effect of aging on the accuracy of visually guided saccadic eye movement. *Annals of Neurology, 16*(4), 449-454.

Wilson, S. J., Glue, P., Ball, D., & Nutt, D. J. (1993). Saccadic eye movement parameters in normal subjects. *Electroencephalography and Clinical Neurophysiology, 86*(1), 69-74.

Winterson, B. J., & Collewun, H. (1976). Microsaccades during finely guided visuomotor tasks. *Vision Research, 16*(12), 1387-1390.

Yang, Q., & Kapoula, Z. (2006). The control of vertical saccades in aged subjects. *Experimental Brain Research, 171*(1), 67-77.

Yuval-Greenberg, S., Tomer, O., Keren, A. S., Nelken, I., & Deouell, L. Y. (2008). Transient induced gamma-band response in EEG as a manifestation of miniature saccades. *Neuron, 58*(3), 429-441.

Zuber, B. L., Stark, L., & Cook, G. (1965). Microsaccades and the velocity-amplitude relationship for saccadic eye movements. *Science, 150*(3702), 1459-1460. doi:

10.1126/science.150.3702.1459

8. List of Abbreviations

AD	Alzheimer's disease
AMD	Age-related macular degeneration
ARVs	Areas of residual vision
BEM	Boundary element method
dCX	Horizontal disconjugacy index
dCY	Vertical disconjugacy index
EEG	Electroencephalogram
EMG	Electromyography
ERPs	Event related potentials
ERSPs	Event-related spectral perturbations
FEF	Frontal eye field
FIR	Finite impulse response
fMRI	Functional Magnetic Resonance Imaging
HRP	High-resolution perimetry
ICA	Independent component analysis
iCoh	Imaginary part of coherence
ITC	Inter-trial coherence
LGN	Lateral geniculate nucleus
MCI	Mild cognitive impairment
MLR	Microsaccadic lambda response
OL	Occipital lobe
PCA	Posterior cerebral artery
PD	Parkinson's disease

PEF	Parietal eye field
PICA	Posterior inferior cerebellar artery
PSP	Progressive supranuclear palsy
ROIs	Regions of interest
SC	Superior colliculus
SEF	Supplementary eye field
SP	Spike potential
V1	Primary visual cortex
VEP	Visually evoked potentials
wMNE	Weighted Minimum Norm Estimate

9. List of Figures

one control subject.

Figure 4.5. HRP visual charts, monocular and binocular microsaccade angular histograms of representative hemianopia cases of the biased (A) and the non-biased group (B).

10. List of tables

11. Curriculum Vitae

Name:	GAO, Ying
Date of Birth:	22.05.1986
Place of Birth:	Jiangsu, China
Gender:	female
Nationality:	Chinese
Professional affiliation:	Institute of Medical Psychology
	Otto von Guericke University of Magdeburg
Email:	ying.gao@med.ovgu.de

Education and Experiences:

08.2013 - 10.2018	PhD candidate under the supervision of Prof. PhD. Bernhard A. Sabel at Institute of Medical Psychology, University of Magdeburg, Germany.
02.2013 - 07.2013	Internship at Department of Neurology, Beijing Tongren Hospital, China.
07.2012 - 01.2013	Research assistant at Institute of Psychology, Beijing Normal University, China.
09.2009 - 06.2012	Master study in cognitive psychology, at Institute of Psychology, Southwest University, China.
09.2004 - 06.2009	Bachelor study in applied psychology, at Institute of Psychology, Southwest University, China.
09.2001 - 06.2004	High school study at Ningbo Middle School, China.
09.1998 - 06.2001	Middle school study at Shuguang Middle School, China
09.1992 - 06.1998	Primary school study at Dongshenglu Primary School, China

Publications:

Gao, Y., Huber, C., Sabel, B. A. (2018) Stable microsaccades and microsaccade-induced global alpha band phase reset across the life span. Investigative Ophthalmology & Visual Science. 59(5): 2032-2041. DOI: 10.1167/iovs.17-23039

Sabel, B. A., Cárdenas-Morales, L., & **Gao, Y.** (2018). Vision Restoration in Glaucoma by Activating Residual Vision with a Holistic, Clinical Approach: A Review. Journal of current glaucoma practice, 12(1), 1.

Dada, T., Mittal, D., Mohanty, K., Faiq, M. A., Bhat, M. A., Yadav, R. K., Sihota, R., Sidhu, T., Velpandian, T., Kalaivani, M., Pandey, R. M., **Gao, Y.**, Sabel, B.A., Dada, R.

(2018). Mindfulness Meditation Reduces Intraocular Pressure, Lowers Stress Biomarkers and Modulates Gene Expression in Glaucoma: A Randomized Controlled Trial. Journal of glaucoma.

Yang, F.H., Dobson, K., Li, X.M., Hennebury, A., **Gao, Y.**, Tang, X. F., & Qi, L. (2018). Cross-Cultural Supervision in Cognitive-Behavioral Therapy: A Case Study. Cognitive and Behavioral Practice. DOI: 10.1016/j.cbpra.2017.12.004

Gao, Y., Sabel, B. A. (2017). Microsaccade dysfunction and adaptation in hemianopia after stroke. Restorative Neurology and Neuroscience. 35(4):365-376. DOI: 10.3233/RNN-170749

Gao, Y., & Zhang, H. (2014). Unconscious processing modulates creative problem solving: Evidence from an electrophysiological study. Consciousness and Cognition, 26(1), 64–73.DOI: 10.1016/j.concog.2014.03.001

Scientific Presentations:

Gao, Y., Sabel, B. A. (2018). Microsaccades reset global alpha band phase and enhance alpha band functional connectivity network efficiency. **Poster presentation** at the 11th FENS Forum of Neuroscience. Berlin, 7-11.07.2018.

Gao, Y., Sabel, B. A. (2017). Microsaccadic alpha band phase resetting – a stable life – long mechanism of cortical refreshment in addition to retinal refreshment. **Oral presentation** at the 4th International Symposium "Low Vision and the Brain". Berlin, 24 – 26.11.2017.

Gao, Y., Sabel, B. A. (2017). Microsaccade features and microsaccade-related alpha-synchronization across the life span. **Oral presentation** at the 19th European Conference on Eye Movements. Wuppertal, 20-24.08.2017.

Sabel, B. A., Gao, Y. (2016). Impaired binocular microsaccades in hemianopia. **Free-paper presentation** at the 31st Asia-Pacific Academy of Ophthalmology Congress in conjunction with the 57th Annual Meeting of the Ophthalmological Society of Chinese Taipei, the European Society of Ophthalmology. Taipei, 23-27.03.2016.

Gao, Y., Sabel, B. A. (2015). Impaired binocular microsaccades in hemianopia. **Poster presentation** at the European Society for Low Vision Research and Rehabilitation (ESLRR). Oxford, 25-27.09.2015.

Gao, Y., Sabel, B. A. (2015). Impaired binocular microsaccades in hemianopia. **E-Poster presentation** at the European Congress of NeuroRehabilitation (ECNR). Vienna, 01-04.12.2015.

Gao, Y., Gall, C., & Sabel, B. A. (2015). Impaired binocular microsaccades in hemianopia. **Poster presentatio**n at the 11th Goettingen Meeting of the German Neuroscience Society. Goettingen, 18-21.03.2015.

Gao, Y., Gall, C., & Sabel, B. A. (2014). Impaired binocular microsaccades in hemianopia. **Poster presentation** at the European Summer School on Eye Movements (ESSEM). Freiburg, 8-13.09.2014.

12. Selbständigserklärung

M.Ed. Ying Gao

+49 17657674515
Ernst-Lehmann-Str. 2/112
39106 Magdeburg
ying.gao@med.ovgu.de

Erklärung

Hiermit erkläre ich, dass ich die von mir eingereichte Dissertation zum dem Thema „**Microsaccades in normal vision and in hemianopia after stroke**" selbständig verfasst, nicht schon als Dissertation verwendet habe und die benutzen Hilfsmittel und Quelles vollständig angegeben wurden.

Weiterhin erkläre ich, dass ich weder diese noch eine andere Arbeit zur Erlangung des akademischen Grades doctor rerum naturalium (Dr. rer. nat.) an anderen Einrichtungen eingereicht habe.

Magdeburg, 23.04.2018

Ying Gao